Testing and manipulating entanglement: nonlocality and purification

Salart Subils, Daniel

UNIVERSITÉ DE GENÈVE
Groupe de Physique Appliquée - Optique

FACULTÉ DES SCIENCES
Professeur Nicolas Gisin

Testing and Manipulating Entanglement:

Nonlocality and Purification

THÈSE

présentée à la Faculté des Sciences de l'Université de Genève
pour obtenir le grade de Docteur ès sciences, mention physique

par

Daniel Salart Subils

d'Espagne

Thèse N° 4200

GENÈVE
Atelier de reproduction de la Section de physique
2010

Abstract

The scope of this thesis is to discuss several experiments related to the quantum phenomenon of entanglement. We start by introducing entanglement and, more specifically, the two forms that we use in our experiments: energy-time entanglement and single-photon entanglement. We explain how entanglement can be created through the process of spontaneous parametric down conversion in non-linear waveguides. We explain the importance of Bell inequalities and how we can use them to put quantum physics to the test.

We describe how we performed three entanglement-related experiments. First, in a Bell experiment with spacelike separation, we explored the possibility that a change in the gravitational field around one of the detection devices could trigger the collapse of the wavefunction, ending the entangled state. Macroscopic massive objects linked to the detection devices were displaced during the measurement to trigger this collapse. No reduction in the visibility of the interference fringes was observed and the correlations violated Bell inequalities. The results reinforce the nonlocal nature of quantum correlations.

Second, we tested the hypothesis that a superluminal signal defined in a universal privileged reference frame travelling between the detectors could influence the results. We tested all possible reference frames aligning our Bell experiment with the east-west direction and maintaining the measurement for more than 24 hours. No reduction in the interference visibility below the threshold set by the CHSH Bell inequality was observed. If this hypothetical influence exists, its speed must be at least 10000 times that of light.

Third, we implemented an entanglement purification protocol using single-photon

entanglement and linear optics elements. We adjusted all the modes of the photons to obtain a high degree of indistinguishability that allowed us to measure a HOM dip with 99,0% visibility. We reduced the entanglement of the created entangled states by introducing noise in the fiber in a controlled way. We measured the fidelity of the entangled states and then we purified these states to obtain a higher fidelity than that of the original states.

Résumé de la thèse

La physique quantique est souvent en contradiction avec notre intuition. Par example, un système quantique peut être dans deux états différents en même temps: c'est le principe de superposition quantique. De même, la dualité onde-corpuscule est surprenant: ce qu'on croyait être une particule peut se comporter comme une onde, et ce qu'on croyait une onde peut aussi se comporter comme une particule. Mais, peut être le phénomène le plus étrange de la physique quantique est celui de l'intrication.

Ce phénomène a été décrit pour la première fois en 1935 par Schrödinger [1] et aussi, pendant la même année, dans un article écrit par Einstein, Podolsky et Rosen [2]. Ces trois derniers proposaient l'expérience *Gedanken* suivante: considérons deux particules qui ont un passé commun mais qui actuellement se trouvent très éloignées l'une de l'autre. Selon la physique quantique, des correlations existent entre les deux particules de sorte que si une mesure est réalisée sur une des ces particules pour en déterminer l'état, alors l'état de la deuxième est aussi instantanément déterminé.

Ceci est complètement contraire à notre vision du monde, dans laquelle un système ne peut avoir un effet sur un deuxième, que si une information se propage entre les deux systèmes. On connait aussi, depuis la théorie de la relativité, qu'aucune information ne peut se propager plus vite que la vitesse de la lumière. Cela implique que, si les systèmes sont separés spatialement, un certain temps doit s'écouler entre les événements vécus par ces systèmes. Le problème centrale semble associé au principe de 'localité'. La localité dit qu'un changement effectué sur un système physique ne peut pas avoir un effet sur un deuxième système separé spatialement du premier. Pour des systèmes quantiques, cette supposition est incorrecte car ces correlations sont nonlocales.

Mais une deuxième possibilité existe qui essaie d'expliquer le caractère de ses corrélations et qui évite d'appeler à la nonlocalité. C'est l'hypothèse que l'état quantique des particules est incomplet et qu'il doit être completé par des 'éléments de réalité' ou 'variables cachées'. En 1964, Bell a proposé des inégalités [3] qui permettent de déterminer si le résultat d'une certaine expérience est explicable par des variables cachées locales. Quelques années plus tard, plusieurs tests de ces inegalités ont été effectués et ils ont prouvé la nonlocalité quantique. Mais même aujourd'hui, il est important de continuer à réaliser des expériences de Bell de plus en plus performantes pour exclure définitivement l'interpretation des variables cachées locales.

Mais l'intrication n'est pas seulement un phénomène curieux, c'est aussi une ressource très utile dans le champ de la communication quantique. Des expériences de cryptographie quantique, de téléportation quantique et bien d'autres encore ont utilisé l'intrication pour encoder et transmettre de l'information. Un des problèmes avec ce type d'experiences c'est la dégradation de l'intrication lors de sa transmission, ce qui limite la distance sur laquelle on peut l'envoyer.

Actuellement une des méthodes potentielles pour distribuer l'intrication sur de longues distances c'est la construction d'un répéteur quantique [4]. Les répéteurs quantiques ont besoin de distribution annoncé et stockage de l'intrication entre des liens élémentaires de distance moderé et successives opérations d'*entanglement swapping* entre les liens. Finalement, la purification permet de corriger les erreurs introduits par les *swappings* successifs.

Dans cette thèse, après une description de l'intrication et des inégalités de Bell on décrit trois expériences dans lesquelles l'intrication est centrale. Dans la première expérience, nous avons réalisé une expérience de Bell avec la supposition que la mesure n'est terminée qu'après qu'un objet de masse macroscopique relié à l'appareil de détection ait bougé. Cette hypothèse établie une relation entre la physique quantique et la gravitation. Nous avons observé des franges d'interférence avec une visibilité supérieure que la limite donné par les inégalités de Bell.

Dans une deuxième experience de Bell nous avons testé l'hypothèse selon laquelle un signal voyageant à une vitesse plus grande que celle de la lumière puisse changer les résultats de la mesure. Cette vitesse doit être définie dans un système de référence

universel privilégié. Pour cela nous avons aligné notre experience de façon que la ligne qui relie nos détecteurs soit parallèle à la direction est-ouest de la Terre. Après 24 heures, la Terre a fait un tour complet est nous avons testé tous les systèmes de référence potentiels. Nous avons établi une limite inférieure pour la vitesse de ce signal au moins égal à 10000 fois la vitesse de la lumière.

Dans une troisième expérience nous avons implementé un protocole de purification d'une intrication de 2 modes ne partageant qu'un seul photon. Nous avons crée deux états intriqués à un seul photon et nous les avons envoyés à deux partenaires séparés par quelques mètres de fibres optiques. Nous avons introduit du bruit dans le système de façon controlé pour réduire l'enchevêtrement des états. Le protocole de purification est implementé avec des coupleurs variables qui combinent les modes des états intriqués. Si un photon est détecté sur un des modes à la sortie des coupleurs, un nouveaux état intriqué est crée par les autres modes avec une fidélité supérieure à la fidélité initiale.

Contents

List of Figures

Chapter 1

Introduction

In our every day experience of the world, to change the state of an object we have to exert some kind of influence upon it. This can be a direct effect, like touching the object, or the product of a long chain of events that eventually reach said object. Even when we attempt to think of an exception, for example, it is possible to communicate with someone who is at the other side of the world through a telephone, we realize that there is an electromagnetic signal that gets transmitted between the phones, and this signal cannot propagate faster than the speed of light. In essence, to change something there must be an influence that gets transmitted from us to the object, and it takes time for this influence to get there. As far as we can tell through our senses, everything behaves this way. It is our intuition of how the world works, and we call this intuition 'locality'.

Back in the 17th century, when Isaac Newton discovered that distant objects are attracted to each other through gravity [8], he could not figure out how gravity was transmitted, so it appeared to violate this 'locality' intuition, and it was called 'action at a distance'. Later, in the 19th century, when electromagnetism began to be understood, it also seemed to be acting at a distance without any intermediary. But in the later part of the same century, the concept of field was introduced, and both gravity and electromagnetism could be explained by the propagation of fields through space. These fields are real and can be measured. So, in the end, there was no 'action at a distance' and both gravity and electromagnetism turned out to be

'local' after all.

In the beginning of the 20th century, quantum physics was discovered. According to the most accepted interpretation of quantum physics, it is possible for two spatially separated particles, that a measurement on one of the particles has an effect on its distant partner instantly and without an intermediary influence. This correlation between the particles does not follow our locality intuition. For the first time, something that can not provenly be explained through some kind of local effect had been discovered. Thus, the conclusion is that quantum correlations are nonlocal. However, despite exhibiting nonlocality, quantum physics is still compatible with the theory of relativity. Particularly, quantum physics obeys the condition of no-signalling, that is, nonlocal correlations between space-like separated locations can not be used for superluminal communication.

Nonlocal correlations are attributed to the phenomenon of entanglement, which is responsible for a good part of the fascination that quantum physics inspires. The term 'entanglement' was first used in this sense by Schrödinger in 1935 [1]. In that same year, Einstein, Podolsky and Rosen, while trying to assert that quantum theory is not complete, came up with the thought experiment about the two correlated particles mentioned above (called the EPR experiment) [2]. Einstein did not believe that entanglement can be held responsible for the correlations. In a somewhat despisable way, he called the instantaneous effect between the particles 'spooky action at a distance'. At that time, there were no means to find out if he was right or not.

Nonlocality is so alien to our intuition that not everyone was convinced by it. A second hypothesis arised that tried to explain the correlations without using nonlocality. This hypothesis says that quantum physics is actually incomplete and it has to be complemented by 'elements of reality' or 'hidden variables' that are present in each quantum state and are therefore local.

In 1964, John Bell realized that the hypothetical existence of local hidden variables could be experimentally tested [3]. If an experiment similar to the EPR experiment was performed, its outcome could be used to calculate the value of a certain parameter. If the correlations between particles were the result of local variables, this parameter could only be as high as the upper bound of the inequalities he had deduced. On

the contrary, if the correlations were nonlocal, the parameter could attain a higher value and violate the inequalities. It was not until 1972, when Freedman and Clauser [9], and then also Alan Aspect in 1982 [10], that the first Bell-type experiments were performed. From those results, it was concluded that quantum theory had passed the test, and that local hidden variables could be excluded. Since then, Bell experiments have been refined and repeated many times but the nonlocality has always been confirmed. However, none of those tests were loophole free, so the interest to continue performing Bell experiments remains, even at the present time.

As explained above, the first approach of quantum physicists towards entanglement was a purely conceptual one. The primary goal was to determine if it was nonlocal or not, to explain its mechanism and to understand it. And this approach continues to be investigated today. However, in the decade of the 80's, physicists began to look at entanglement as a new type of physical resource that could be exploited, rather than just some weird property that had to be explained away. This view became more widespread in the 90's, when it was realized that entanglement could be manipulated and several applications were found for it: quantum cryptography [11] and quantum teleportation [12] among others. These operations usually involve the distribution of quantum states to distant locations through quantum channels.

In general, quantum communication channels contain 'noise', which reduces the fidelity of the transmitted quantum states. This noise can be present in the form of phase errors if the quantum states are phase-dependent. Therefore, quantum communication would be limited to short distances if it were not for quantum teleportation, entanglement swapping and entanglement purification protocols. These protocols combined can be used to build a quantum repeater [4] which would lengthen the distance that can be reached with quantum communication.

In quantum teleportation, two photons belonging to the same entangled state are distributed to distant locations where one of them interacts with the quantum state that we wish to teleport. Then, through a combination of nonlocal correlations and classical communication, the information of this state is 'transmitted' to the other entangled photon. Furthermore, in entanglement swapping protocols [5], through the interaction of two photons belonging to two different entangled states, the other two

photons of these states can be projected into a new entangled state, even though they share no common past. It can be said that this makes possible the teleportation of entanglement itself.

In a quantum repeater, entanglement swapping operations distribute entanglement between short distance elementary links. Entanglement is then stored at the nodes between the links through the use of quantum memories [6], that allow to store and retrieve quantum states. Noise in the communication channels and imperfections in the swapping operations introduce errors, changing a maximally entangled state into a mixed state with a certain entanglement fidelity. Fortunately, entanglement purification protocols [7] allow to correct these errors, combining poorly entangled states to obtain higher entangled ones, at the cost of reducing the number of available entangled states.

The main topic of this thesis will be entanglement. We start with an explanation of entanglement and we will focus on the two forms of entanglement that are most relevant to this thesis: energy-time entanglement and single-photon entanglement. We will describe how we can create entanglement through the process of spontaneous parametric down conversion in non-linear waveguides. We will dedicate chapter 3 to talk about Bell inequalities and Bell-type experiments. Then, we will describe in detail the three experiments that were performed during this thesis.

In the experiments described in chapters 4 and 5, we close two of the remaining loopholes of Bell experiments as well as increasing the separation between the parties. In the first experiment, we test the hypothesis that says that the collapse of the wavefunction is linked to gravitation. We performed a Bell experiment where two photons are sent to spacelike separated locations. The detection of a single photon triggers the displacement of a macroscopic massive object. The spacelike separation takes into account the time of measurement which includes the time to displace the massive object. In the second experiment, we analyze the possibility that a superluminal influence could travel between the two detection locations and change the outcome of the experiment. Ensuring that the two detections take place simultaneously and aligning the axis of the experiment with the east-west direction, we test all possible reference frames and find a lower bound for the speed of this superluminal influence.

In the experiment described in chapter 6, we use, for the first time, a purification protocol to purify single-photon entangled states. We first create two entangled states, each one consisting of two modes sharing one photon. One mode from each state is distributed to one of two different partners who perform a linear unitary transformation on them using linear optics elements. The transformations consist in combining the modes with variable ratio couplers with a particular transmission/reflection ratio. Conditional on the detection of only one photon at one of the couplers outputs, a purified entangled state is created.

The research performed during this thesis has contributed to confirm entanglement as a nonlocal phenomenon and hopefully has paved the way to one day perform a loophole free Bell experiment. On the other hand, the first experimental test of single-photon entanglement purification has proved the feasibility of a protocol that one day could be applied in a long-distance quantum repeater.

Chapter 2

Entanglement

A bit is the smallest unit of logic information that exists. For a system that can exist in two different states, a bit is all that is needed to know in which state it is. It can be represented by any two symbols, but it is usually represented by a 0 and a 1.

A qubit is the quantum equivalent of the classical bit. A qubit also gives information about the state of a system but, because it is a quantum system, it can be in a superposition of both states. It is usually represented by $a|0\rangle + b|1\rangle$, where $a^2 + b^2 = 1$ and a^2 and b^2 are the probabilities of the system being in states $|0\rangle$ and $1\rangle$, respectively.

In quantum communication, qubits can be used to send information. In these cases, it becomes necessary to encode the qubits in a physical system. Different physical systems exist that are suitable to encode qubits: atoms, ions and quantum dots are some common examples. But if we want to send the information to a distant location, the most suitable one is the photon. In the experiments described in this thesis, we use photons to encode qubits and we use optical fibers to send the photons to distant locations. We also use entanglement to manipulate the qubits and obtain results that would not be possible if we were using classical bits and classical communication.

Entanglement is the phenomenon by which a pair or more particles (for example, photons) can be in a definite state while each of them is in a mixed state. An example of an entangled state for two qubits is

$$|\Phi\rangle = \frac{1}{\sqrt{2}}(|0\rangle_A|1\rangle_B + |1\rangle_A|0\rangle_B) \tag{2.1}$$

A and B design different modes which can correspond, for example, to two different locations. The state of the individual qubits can not be described by separate states. They are in a superposition state where each of them has a 50% chance of being in the state $|0\rangle$ and 50% of being in the state $|1\rangle$. However, if the qubit of mode A is found to be in state $|0\rangle$, then there is 100% certainty that the qubit of mode B is in state $|1\rangle$ (or viceversa).

Different forms of entanglement exist. Most forms involve a pair of correlated particles. We need a form that is strong against decoherence in optical fibers, which we extensively use in our experiments. The most suitable form is energy-time entanglement [13], which is explained in section 2.1. An alternative suitable form would be time-bin entanglement [14]. In this form, photon pairs are created in a coherent superposition of two different emission times. It is well suited for experiments that require joint measurements between photons from different pairs, where the time of creation of each pair must be well defined. Since our experiments do not require this information, we use the slightly less complicated to prepare energy-time entanglement.

2.1 Energy-time entanglement

To understand how energy-time entanglement is created, consider a 3-level atomic system as the one shown in Figure 2.1. An atom is excited to the higher state (state 1) which has a relatively long lifetime τ_1. After emission of a photon γ_1, the atom will be in the intermediate state (state 2), with a much shorter lifetime τ_2 ($\tau_2 \ll \tau_1$). A second photon γ_2 will be emitted very soon after γ_1. The lower state (state 3) has either a long lifetime or is a ground state.

The time at which either photon is emitted is uncertain over a large interval τ_1. However, since both photons are emitted at times that are the same within a small uncertainty τ_2, once one of the photons is detected it determines the relative time

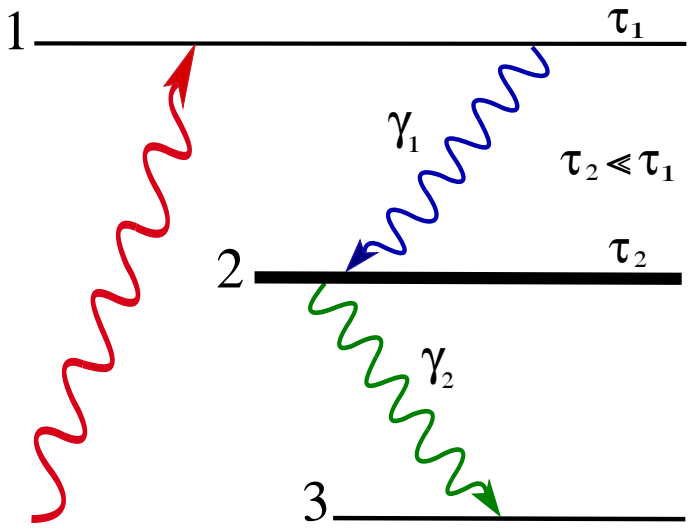

Figure 2.1: Three-level atomic system. State 1 has a much longer lifetime τ_1 than lifetime τ_2 of state 2.

of emission of the other photon with a small uncertainty. Following the energy-time uncertainty principle ($\Delta t \Delta E \geq \hbar/2$), the longer a particle's lifetime is, the smaller the uncertainty of the measured energy will be. The long lifetime of the highest level implies a small uncertainty in the energy of the emitted photon γ_1. On the other hand, γ_2 photons emitted by the intermediate level will have uncertain energies due to short lifetimes. Thus, the energy and the time of emission of each particle are uncertain, but the sum of the energies and the difference of the times are well determined.

Energy-time entanglement can be created through the process of spontaneous parametric down conversion (SPDC) that can take place in a non-linear crystal if the appropriate conditions are met (see Section 2.2). A pump photon creates two photons at the same time within an uncertainty ΔT. This uncertainty is within the long coherence time of the pump photon (equivalent to the long lifetime τ_1 of the highest energy level), whose well-defined energy is shared between the two created photons with short coherence times (equivalent to the short lifetime τ_2 of the intermediate level). This pair of photons will then exhibit energy-time entanglement.

Energy-time entanglement was first proposed by Franson in 1989 [15]. It was experimentally demonstrated in 1992 by Brendel [16] and the following year by Kwiat

[17]. We used energy-time entanglement in the experiments described in chapters 4 and 5 of this thesis.

2.2 Non-linear waveguides

Energy-time entanglement can be created through the process of spontaneous parametric down conversion (SPDC) [18] in nonlinear crystals. This process is more efficient if the light beam is confined in a small area for the entire length of the crystal. For this reason, often a waveguide is used instead of just a bulk crystal. In our experiments, we always used non-linear waveguides based on lithium niobate ($LiNbO_3$).

When light interacts with matter, the photons can be absorbed by the atoms, exciting the electrons that will, eventually, return to their normal state reemitting the photons. For most materials, this reaction is a linear process: the reemitted field is the same as the incident field. However, for non-centrosymmetric materials, if the incident light is intense enough, the incident electric field $\vec{E}$ can induce a polarization $\vec{P}$ in the material that depends non-linearly on the electric field in the following way

$$\vec{P}(\vec{E}) = \epsilon_0 \chi^{(1)} \vec{E} + \epsilon_0 \chi^{(2)} \vec{E}\vec{E} + \epsilon_0 \chi^{(3)} \vec{E}\vec{E}\vec{E} + ... \tag{2.2}$$

where ϵ_0 is the vacuum permittivity and χ is the electric susceptibility. During this thesis, we will only consider up to the second-order susceptibility tensor $\chi^{(2)}$.

In this type of interaction, light of a certain wavelength is converted into other wavelengths. Different combinations of wavelengths are possible, depending on the incident wavelength and the parameters of the material, as long as the conservation of energy is respected. On the particular case where an incident photon of defined wavelength (pump photon) is converted into two photons of longer wavelength (signal and idler photons), the conservation of energy can be expressed as follows

$$\omega_p = \omega_s + \omega_i \tag{2.3}$$

where ω_p, ω_s and ω_i are the wavelengths of the pump, signal and idler photons,

respectively.

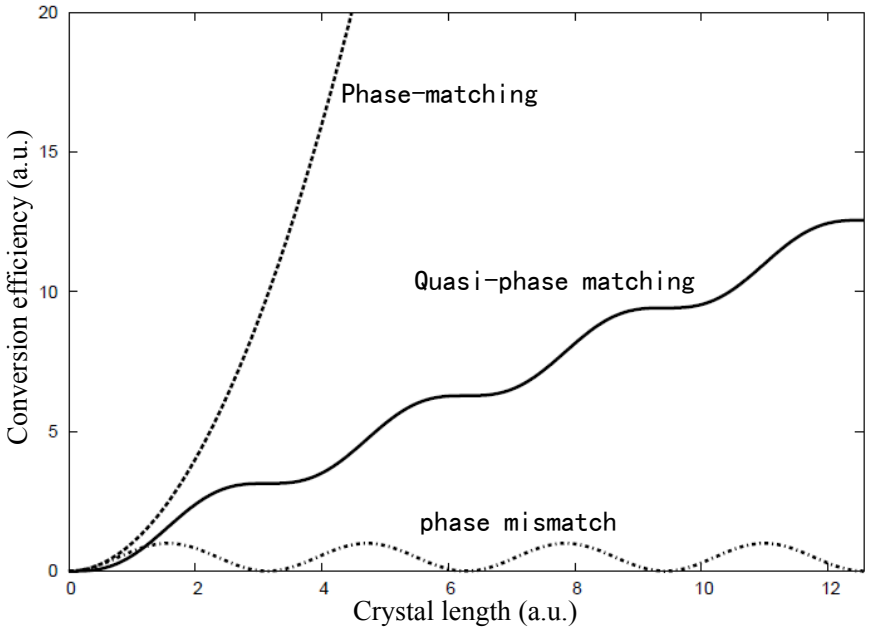

Figure 2.2: Conversion efficiency in a non-linear crystal increases with the length of the crystal if the condition of phase matching is met. For quasi-phase matching, the efficiency also grows but at a lower rate. If there is no phase match, the intensity of converted light oscillates with a period equal to the coherence length, never achieving much power because of destructive interference.

The phase velocity of a photon depends on its wavelength. In a nonlinear crystal, photons with different wavelengths will have different phase velocities because of the dispersion of the material. The pump, signal and idler photons will accumulate a phase mismatch. After a certain length of the crystal, this phase mismatch implies that the light that is created at one point of the material is destroyed at another point by destructive interference. Thus, the efficiency of the conversion is limited. In order to obtain a good conversion efficiency from this process, the phase-matching condition must also be fulfilled.

In birefringent materials, the ordinary and extraordinary axis of the crystal have different refraction index, which implies different velocities of the photons. These materials can be cut at a specific length and angle where the effect of the dispersion

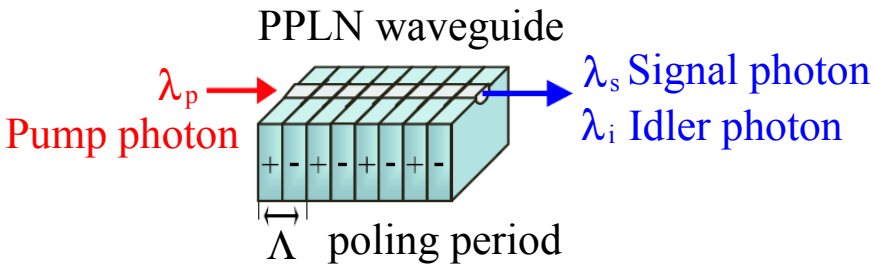

Figure 2.3: Scheme of a periodically poled waveguide.

is reduced so it becomes possible to achieve the phase-matching condition. This method has the disadvantage of not always being able to use the highest non-linear coefficient of the material (d_{31} for $LiNbO_3$). Additionally, it is especially difficult to perform in waveguides as the incidence angle to the crystal is zero.

A different method, demonstrated for the first time in 1962 [19], is the quasi-phase matching condition. The sign of the non-linear coefficient $\chi^{(2)}$ is periodically inverted to compensate for the dephasing accumulated along the direction of propagation of the light. This method is usually applied in a substrate of lithium niobate, so it receives the name of periodic poling lithium niobate or PPLN.

Consequently, in addition to equation 2.3, the pump, signal and idler photons must also accomplish,

$$\frac{n_p}{\lambda_p} = \frac{n_s}{\lambda_s} + \frac{n_i}{\lambda_i} + \frac{1}{\Lambda} \tag{2.4}$$

where n are the indexes of refraction, λ the wavelengths and Λ is the length of the periodic step in the crystal.

The length of the periodic step determines the range of possible wavelengths for each crystal. This method has the advantage of being able to use the highest non-linear coefficient (d_{33} for $LiNbO_3$) but it comes with a lower efficiency rate than the phase-matching condition (as shown in Figure 2.2). The efficiency of SPDC in a typical bulk crystal is on the order of 10^{-12}, while in a typical waveguide of periodically poled lithium niobate, it can attain an efficiency of approximately 10^{-6} [18].

2.3 Single-photon entanglement

In single-photon entanglement, a qubit is not encoded by a particle (a photon) but by a mode of the electromagnetic (e.m.) field. The role of the two entangled particles is played by a photon in a superposition of being at A and B, where A and B represent the photon being at locations A and B, respectively.

An entangled state where a single particle is shared between two modes can be expressed as

$$|\Psi\rangle_{A,B} = |1\rangle_A|0\rangle_B + |0\rangle_A|1\rangle_B \tag{2.5}$$

where $|0\rangle_{A,B}$ and $|1\rangle_{A,B}$ denote Fock states with 0 particles (a vacuum state) and 1 particle, respectively. A and B represent two different modes of the e.m. field.

The nonlocality of a single photon was first introduced by Albert Einstein. In 1991, entanglement involving a single particle (a photon) instead of a pair of correlated particles was first proposed [20]. Single-photon entangled states have been used in quantum teleportation [21] and Bell experiments [22]. Furthermore, entanglement between four modes sharing a single photon has been characterized by direct measurements of the optical modes [23].

In spite of this, some controversy arised [24] around whether there is entanglement in the state represented by equation 2.5. Mapping single-photon entanglement into two atomic ensembles and revealing the entanglement between these ensembles solved part of the controversy [25].

If the particle is a freely propagating photon, single-photon entanglement can be created sending a single photon through a beamsplitter. We used single-photon entanglement in the experiment described in chapter 6 of this thesis.

Chapter 3

Bell experiments and Bell inequalities

As mentioned in the Introduction, it is commonly accepted that since quantum correlations do not follow our locality intuition they are thus nonlocal and attributed to entanglement. A different view holds that quantum theory might be incomplete and that local hidden variables could exist and actually be responsible for the observed correlations. This second possibility could not be scientifically ruled out until the discovery of Bell inequalities by John Bell in 1964 [3]. The Bell inequalities are a set of equations that allow to determine if quantum correlations can be explained by local hidden variables. Many different Bell inequalities exist but, for the experiments described in this thesis, we will only make use of the Clauser-Horne-Shimony-Holt inequality (CHSH) [26], which is explained in section 3.2.

The Bell inequalities allow to calculate the Bell parameter, through the results of a Bell-type experiment (see Section 3.1). A Bell parameter that violates the inequalities indicates that the correlations cannot be explained by local theories, thus proving that the correlations are definitely nonlocal. Many Bell experiments have been performed since 1972 [9, 10, 27, 28] and the results support the nonlocality of quantum correlations.

The first Bell experiments involved only photons. Since then, violations of Bell inequalities have been observed in massive particles like protons [29] and ions [30],

and even in atomic ensembles [31].

Bell experiments are based on reasonable assumptions about the nature of the correlations but, however small, the possibility that any of these assumptions is false remains. The ultimate goal of Bell experiments is the realization of an experiment whose interpretation does not rely on any assumption besides locality. Unfortunately, the technological challenge that this supposes is too much for today's experimental capability. For this reason, even nowadays Bell experiments continue to be performed in order to close the remaining loopholes one by one.

The two most commonly referred loopholes are:

Detection loophole: due to limited detection efficiency it is not possible to discard the possibility that the sample of detected events is just a selection that replicates the violation of Bell inequalities. This includes the efficiency of the detectors as well as all the losses that might occur since the particles are emitted until they are detected. This loophole has been closed in experiments involving trapped ions thanks to high detection efficiencies and deterministic preparation of an entangled state [30, 32].

Locality loophole: the analyzers and detection devices must be located at spacelike separated locations, in order to avoid an hypothetical signal travelling from one analyzer to the other before the second measurement is completed. Technical challenges limit the achievable distance between the source and the analyzers. In a related note, in order to test if the correlation decreases with the distance, the separation between the source and the analyzers should be increased. This loophole has been closed in experiments involving photons [33, 34] with an ever increasing distance, reaching as far as 10 km [35].

Two other loopholes that are of particular interest for this thesis are the one related to the gravitational collapse of the wavefunction, which we will explain in chapter 4, and the one related to the superluminal signalling between detection events, which we will discuss in chapter 5.

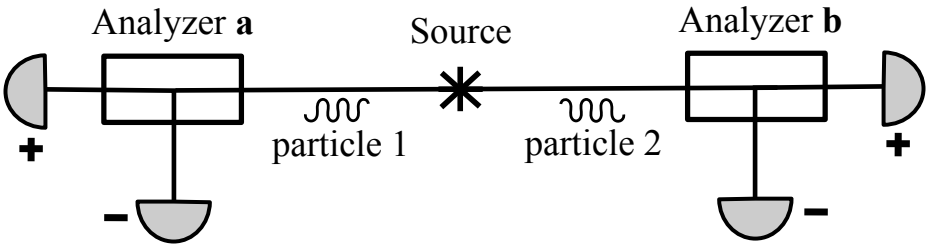

Figure 3.1: Scheme of a Bell experiment. Depending on the parameter's position at analyzer **a**, particle **1** will be detected at detector + or detector **-**. Because of the correlation, this will effect in which detector particle **2** is detected.

3.1 Bell experiments

Setting aside differences particular to each experiment, in general, a Bell experiment is performed as follows. Pairs of correlated particles are created, for example, by the process of spontaneous parametric down conversion described in the precedent chapter. Each particle of the pair is sent to a separate analyzer device and then detected, as shown in Figure 3.1. The analyzer controls a parameter whose position can be shifted to change the outcome of the particle. In the case of energy-time entanglement, that would be the phase shift of an interferometer, in the case of polarization entanglement, the polarizers orientation. Because of the correlation, what the analyzer does to a particle has an influence on the outcome of its pair. The results are then analyzed to calculate the Bell parameter.

3.1.1 Franson experiment

A Franson experiment [15] is a type of Bell experiment where the analyzers are interferometers with arms of different length. As shown in Figure 3.2, a 50/50 beamsplitter is used to send photon 1 (2) either through the short arm S_1 (S_2) or the long arm L_1 (L_2). The two paths recombine at a second 50/50 beamsplitter and then the photons are detected.

The path length difference between the short and the long arms must be the same for both interferometers. Thus, the difference in the time of arrival ΔT is the

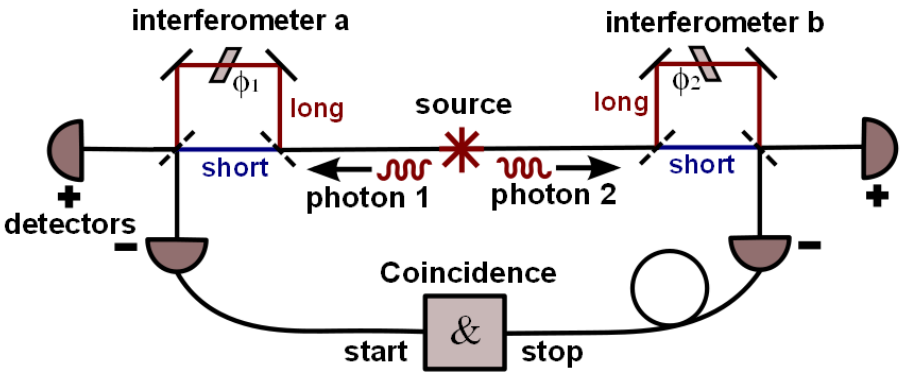

Figure 3.2: Scheme of a Franson experiment.

same for both photons if both choose the same arm. In accordance with what we said in section 2.1, this time must be much shorter than the coherence time of the pump laser (τ_1) but much longer than the coherence time of the created photons (τ_2) ($\tau_2 \ll \Delta T \ll \tau_1$). This is to ensure that there is fourth-order interference if both photons choose the same arm but no second-order interference (i.e. single-photon interference) between the different paths of the same interferometer. The phase of the interference (ϕ_1 and ϕ_2) can be shifted through a device that slightly changes the length of one arm.

After the photons are detected, the information about the time of detection and in which detector it has occurred is registered and then analyzed by a coincidence electronics system. A certain number of time-correlated events (coincidences between the particles time of arrival) is accumulated over a period of time. A graph like the one shown in Figure 3.3 is obtained. The left and right peaks correspond to the photons choosing different arms. The central peak corresponds to both photons choosing the same arm (either both short or both long). The number of events per period of time in the central peak depends on the relative phase of the interferometers ($\phi_1 + \phi_2$) because of fourth-order interference. Scanning this phase, allows to observe interference fringes whose visibility can be used to calculate the Bell parameter, as we will see in the next section.

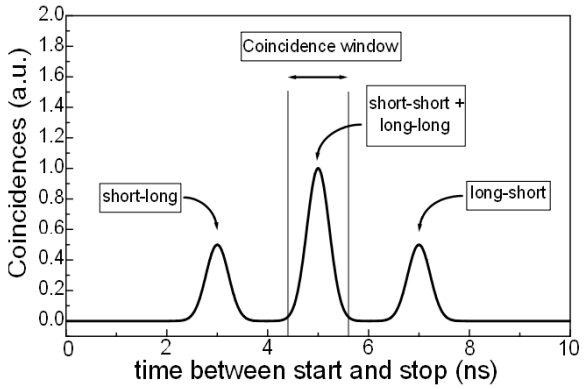

Figure 3.3: Distribution of coincidences by the difference in the time of arrival.

3.2 Bell inequalities: CHSH

One of the most frequently used forms of the Bell inequalities is the Clauser-Horne-Shimony-Holt (CHSH) Bell inequality [26]. Assuming local theories, this inequality has a Bell parameter of

$$S = |E(a,b) + E(a,b') + E(a',b) - E(a',b')| \leq 2 \tag{3.1}$$

where $E(a,b)$ is a correlation coefficient and a, b are the parameters for each analyzer. In a Franson experiment, a and b are values for the phase of the interferometers.

The correlation coefficient can be written as

$$E(a,b) = \frac{R_{++}(a,b) - R_{+-}(a,b) - R_{-+}(a,b) + R_{--}(a,b)}{R_{++}(a,b) + R_{+-}(a,b) + R_{-+}(a,b) + R_{++}(a,b)} \tag{3.2}$$

where $R_{+-}(a,b)$ is a coincidence function that gives the number of coincidences between detector $+$ at analyzer a and detector $-$ at analyzer b.

The coincidence function gives us the coincidence count rate and is given by

$$R_{i,j}(a,b) \propto (1 + ijVcos(a+b)) \tag{3.3}$$

where $i, j = \pm$ and V is the visibility of the interference fringes defined as

$$V = \frac{R_{max} - R_{min}}{R_{max} + R_{min}} \tag{3.4}$$

where R_{max} and R_{min} are the maximum and minimum coincidences rates, respectively. Ideally, we would obtain $V = 1$. However, due to experimental imperfections this value is usually lower than 1.

The correlation function 3.2 can be combined with equation 3.3 to obtain

$$E(a,b) = Vcos(a+b) \tag{3.5}$$

where $a + b$ is the relative phase of the interferometers.

Setting the parameters $a = 0$, $a' = \pi/2$, $b = \pi/4$, $b' = -\pi/4$, the CHSH inequality yields a Bell parameter,

$$S = 2\sqrt{2}V \tag{3.6}$$

If the visibility is $V \geq 1/\sqrt{2} \approx 71\%$, this value is higher than the one predicted by local theories, implying that the correlations are nonlocal.

Chapter 4

Gravitationally-induced wavefunction collapse

We performed a Bell experiment with spacelike separation between the two parties taking into account the hypothesis that the measurement time is related to gravity-induced state reduction [36].

4.1 The time of measurement

At present, a clear and definitive explanation to the problem of when a quantum measurement is finished does not exist. So far, several hypothesis have been proposed to explain this phenomenon, each one according to a different interpretation of quantum physics. To mention a few, one of them says that a quantum measurement is finished once the result is secured in a classical system [37], another states that the result has to be released in the environment [38], and still another claims that the measurement never finishes [39]. So far, no experiments have been able to solve this problem.

The hypothesis that centers our attention is not one of the above but the one that claims that the collapse of the wavefunction that finishes the measurement is triggered by the variation of the local gravitational field around the measurement device. This hypothesis is supported among others by Penrose [40] and Diósi [41] (see also the useful review [42]). This proposal assumes a link between quantum physics

and gravity. The idea is that space-time gets in a superposition of states depending on the configuration of some massive object linked to the measurement device. As soon as this massive object moves, it changes its surrounding gravitational field, and the wave-function collapses ending the measurement.

The time that it takes for the wavefunction to collapse is, according to Diósi (Penrose's equation only differs by a factor of 2),

$$t_D = \frac{3\hbar V}{2\pi G m^2 d^2} \tag{4.1}$$

where V is the volume of the moving object, m is its mass and d is the distance it has moved.

Previous Bell experiments have assumed that the measurement is finished as soon as the photons are detected. No macroscopic massive object was linked to the measurement device. The only displacement of mass involved in this kind of experiments is that of the avalanche of electrons that occurs in the photodiodes, not near enough as massive as necessary to test this possibility. According to this hypothesis, it was realised by Kent [43] that no tests so far have been really spacelike separated, in the sense that they do not exclude the possibility that some kind of signal could travel between the two detection stations influencing the results and leading to the violation of Bell inequalities before the measurement is finished.

4.2 Experimental setup

The experimental setup is that of a Franson experiment [15] with the detection stations separated by 18 km, which is a record distance for this kind of experiments [27, 28]. The source is situated at the center and the photons travel through the installed commercial network (Swisscom) of optical fibers. Each detector is linked to a different macroscopic massive object that move every time that a photon is detected.

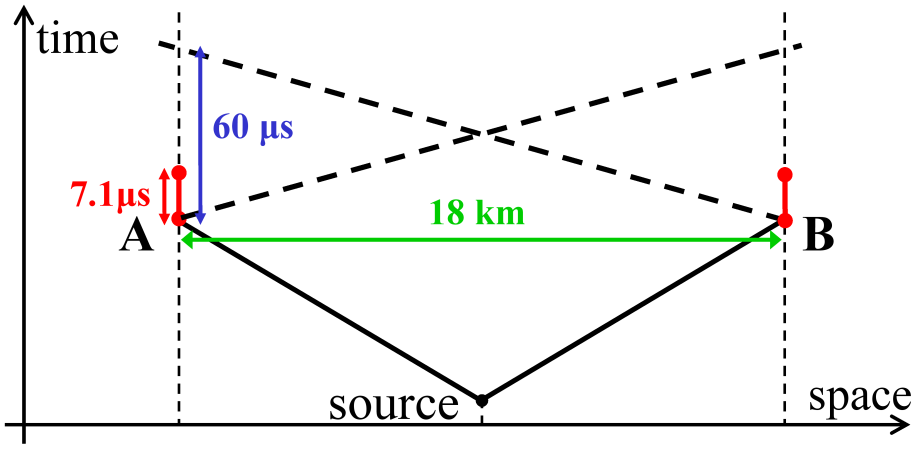

Figure 4.1: Space-time diagram of the experiment. Solid black lines are photons sent from the source to points A and B. Red lines are the times of measurement and are much shorter than the time it takes the hypothetical signals (dotted lines) to travel from A to B (or viceversa) at the speed of light. Therefore, A and B are spacelike separated.

4.2.1 The macroscopic massive object

The macroscopic massive objects are two piezoelectric actuators (PI, PL033) of 3x3x2 mm in size and weighing 140 mg. Every time that an avalanche is triggered at one of the single-photon detectors, a step voltage is sent to the corresponding piezo. The displacement of the piezo is verified by the use of a bulk Michelson interferometer and a golden-coated mirror of 3x2x0.15 mm in size and weighing 2 mg that we attached to one of the surfaces of the piezo.

The interferometer consists of an He-Ne laser ($\lambda = 633nm$) directed to a beam-splitter (BS) and the tiny mirror attached to the piezo placed at the end of one of the arms. The light exiting through one of the outputs of the interferometer is detected by a photodiode. The voltage coming out of the photodiode is proportional to the intensity of light detected and is monitored using an oscilloscope. When the voltage applied to the piezo is zero, the light intensity remains constant. As soon as a step voltage is applied to it, a change in the voltage is observed, indicating that the phase of the interference fringe has changed and thus that the mirror has moved.

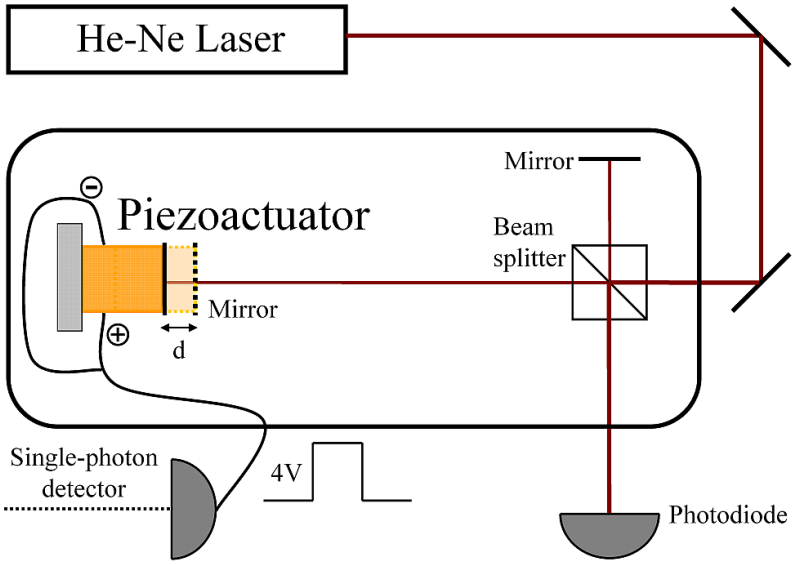

Figure 4.2: Scheme of the bulk interferometer set to verify the displacement of the piezo actuator. A 4V step voltage is applied to the piezo each time an avalanche is triggered at the single-photon detector. The mirror displacement produces interference fringes observed by the photodiode.

To ensure spacelike separation, the measurement time (t_m) must be much smaller than the time the light needs to travel between the detection stations (18 km). This latter time is $t_t = 60\mu$s. The time of measurement consists of the time of collapse (t_D) plus the time needed to move the piezo. The time of collapse was calculated using equation (4.1) and is $t_D = 1\mu$s. The time lapse from the moment the photons are detected until the step voltage reaches the piezo is 0.1 μs. The time from the moment the voltage reaches the piezo until it moves an arbitrary distance d (where d $\approx$ 13 nm) is 6.0 μs. Adding these three times, we obtain a total time of measurement $t_m = 7.1\mu$s. This is almost one order of magnitude smaller than t_t, so we can be certain than the detection stations are spacelike separated.

4.2.2 The Bell experiment

The Bell experiment is performed using a pair of energy-time entangled photons created from a non-linear waveguide pumped with a laser diode. The laser is a

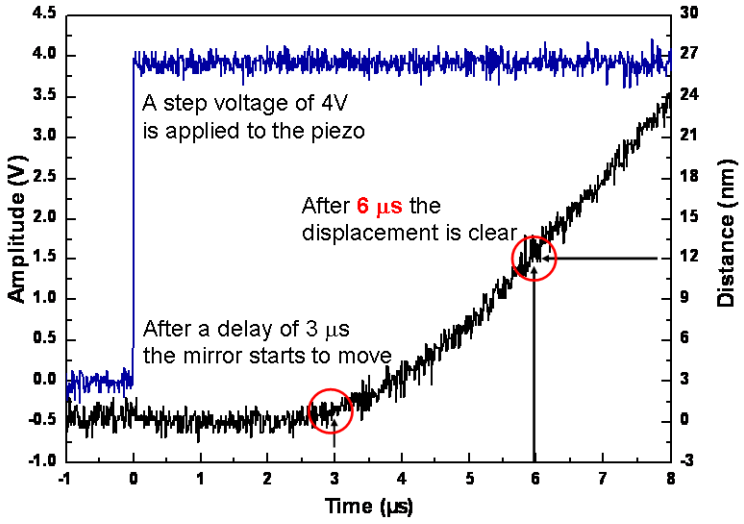

Figure 4.3: Step voltage applied to the piezo (grey line) and consequent change in the intensity of light detected by the photodiode because of the expanded piezo (black line) as measured by the oscilloscope.

continuous wave single mode external cavity diode laser (2.7 mW of power at at a wavelength of 785.2 nm). The waveguide is a periodically poled lithium niobate ($LiNbO_3$, PPLN) type-I waveguide [44]. The created photons have a wavelength around 1550 nm, chosen because the losses in a fiber are relatively low around this wavelength. After the waveguide, some light from the pump laser still remains but it is filtered using a Silicium filter (F) that blocks light at wavelengths shorter than 800 nm.

The pairs of photons are coupled into a monomode optical fiber and then separated using two circulators (C) and two Fiber Bragg Filters (FBG) as shown in Figure 4.5. The first FBG has a central wavelength of 1567.8 nm and a width of 1 nm and the second FBG has a wavelength of 1573 nm with the same width as the

first. Each photon is sent through a 17.5 km long optical fiber to the corresponding detection station situated in the villages of Satigny and Jussy, in the vicinity of Geneva. There, each photon goes through an unbalanced Michelson interferometer and is finally detected by a single-photon avalanche photodiode (APD: idQuantique, id200).

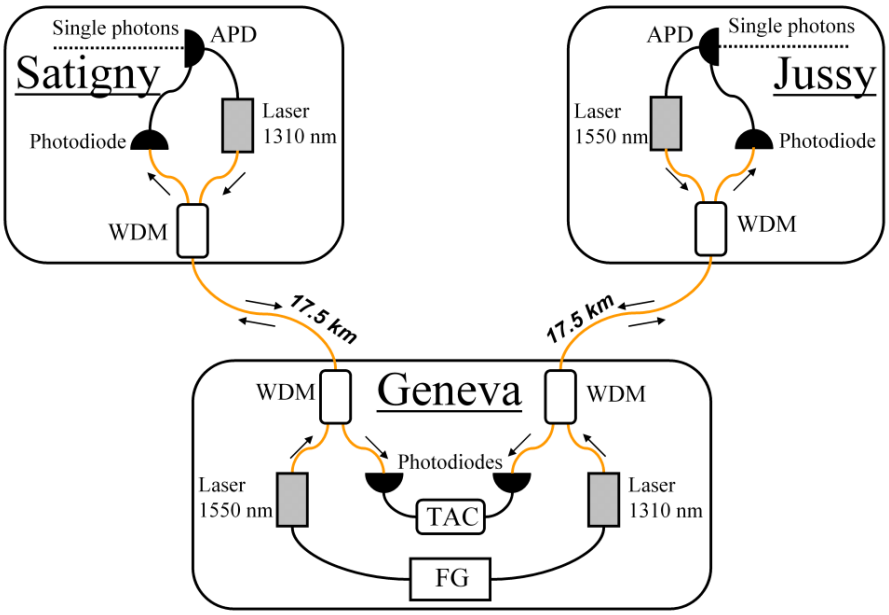

Figure 4.4: Experimental setup to send the classical signals between Geneva and the detection stations.

The detectors work in gated mode [45]. They are both triggered with the same signal sent from Geneva to each detection station through optical fibers (see Figure 4.4). This increases the detection rate of coincidence events. The same optical fibers are used to sent a signal back to Geneva every time that a single-photon is detected. Wavelength division multiplexers (WDM) are used to combine and separate the counter-propagating signals.

As explained in section 3.1.1, if both photons choose the same interferometer arm (which will happen half of the time), it is not possible to determine which one they have taken (the short or the long), producing interference fringes when the relative phase of the interferometers is scanned. The interferometer arm-length difference is

267 mm. This length was selected so as to be shorter than the coherence length of the pump laser ($\approx$ 20 m), and at the same time longer than the coherence length of the single photons ($\approx 2.5mm$), thus avoiding any single-photon interference.

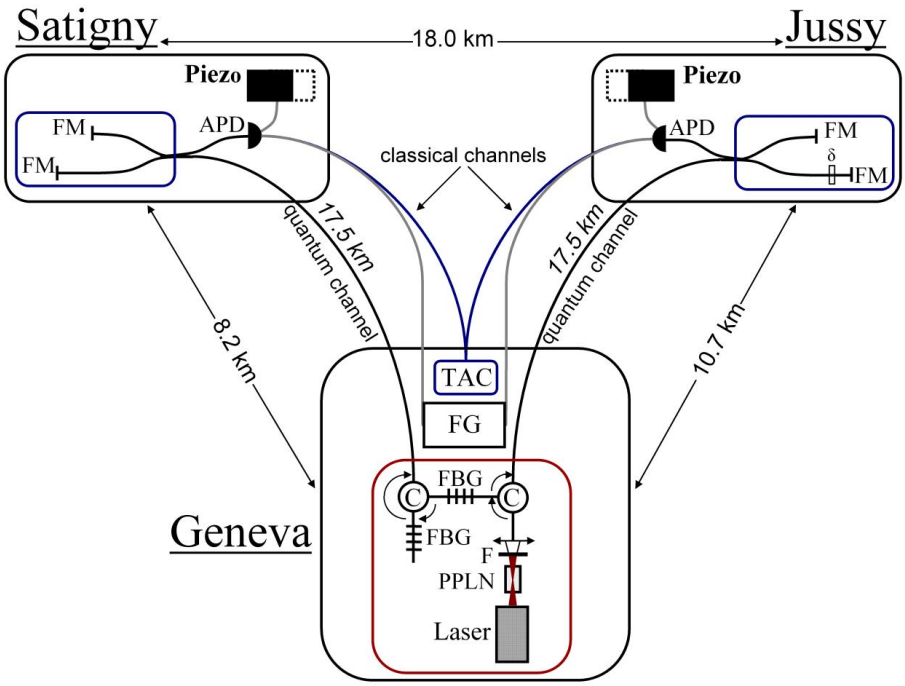

Figure 4.5: Bell experiment setup.

The interferometers have Faraday mirrors (FM) at the end of their arms to compensate for polarization fluctuations [46]. The phase of the interferometers can be changed using temperature controllers. One of the interferometers is kept at a stable temperature and thus at a stable phase for the entire experiment, while in the other the phase (δ) is scanned through a wide range of temperatures to look for interference fringes at its output. Because the two photons are entangled, the change induced in one of them has an immediate effect on its pair.

4.3 Results and conclusion

While scanning the phase, we looked for coincidences in the time of arrival of the photons using a coincidence electronics system. We observed interference fringes with a raw visibility of $V_{raw} = (90.5 \pm 1.5)\%$ (see Figure 4.6), leading to $S_{raw} = 2.56 \pm 0.04$, that is 13 standard deviations (σ) above the threshold given by the Bell inequalities. After subtracting the accidental coincidences, the visibility rises to $V_{net} = (96.7 \pm 1.4)\%$ leading to $S_{net} = 2.74 \pm 0.04$, violating the Bell inequalities by 18σ.

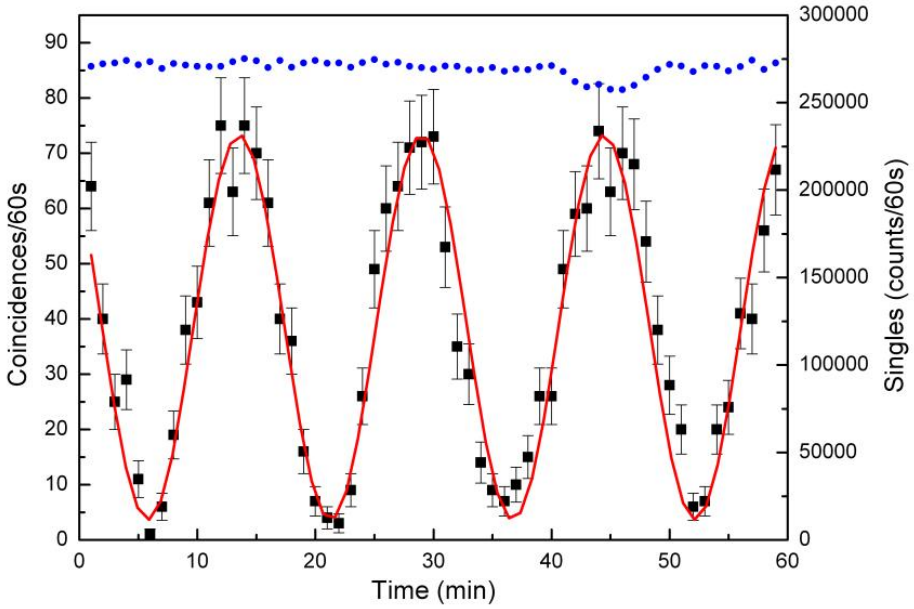

Figure 4.6: Interference fringes with a visibility of $V = (90.5 \pm 1.5)\%$ observed while the piezo was moving.

In conclusion, looking at coincidence events between spacelike separated detection stations, we observed interference fringes with a visibility that violates the Bell inequalities. Our definition of spacelike separation includes that the measurement is finished only after two macroscopic objects, each one linked to one of the detectors, have moved. If gravity is to play a role in the collapse of the wavefunction, for its effects to be measurable a bigger mass than the one used in this experiment

is needed. More likely though, these results just reinforce the nonlocal nature of quantum correlations.

Chapter 5

Speed of quantum information

In the experiment explained in chapter 4, we observed a correlation violating Bell inequalities between detection events taking place at two spacelike separated locations. It is concluded from those results that it is not possible for a signal travelling at the speed of light to cover the distance between the two detection stations before the measurement has finished. That experiment did not discard though the possible existence of a signal that travels faster than the speed of light. We present here an experiment [47] to test this hypothesis.

5.1 The privileged reference frame

If this signal exists, its speed has to be defined in some hypothetical universal privileged reference frame. As realized by Eberhard in 1989 [48], the existence of such a privileged reference frame can be experimentally tested. It is natural to assume that the speed of this hypothetical signal must be finite, so if two events are simultaneous it becomes impossible for the signal to travel between the two. Simultaneity has to be defined with respect to a reference frame, and the events that are simultaneous with respect a certain frame might not be so for a second one moving with respect to the first.

Let's imagine a Bell experiment where the two detection events occur simultaneously with respect to the reference frame of the laboratory. They will also be simultaneous in all reference frames that move in a direction perpendicular to a straight line between the events. But they will not be simultaneous in other reference frames that move in any other direction. As proposed by Eberhard, to be able to test this hypothesis with respect to all possible privileged reference frames we should align the axis of our experiment along the east-west axis of the Earth. After a period of 12 hours, the Earth would have performed half of a rotation and all hypothetical privileged frames would have been tested (see Ref. [49] for more details).

If at some moment of the measurement, the correlation between the detectors disappears or at least, diminishes below the threshold established by the Bell inequalities, we would have found this hypothetical privileged frame. On the contrary, if the correlations are maintained during the whole measurement, we would be able to set a lower bound on the speed of this hypothetical influence. The value of this bound will depend on the uncertainties of the experiment but it will be greater than the speed of light (for spacelike separated events).

5.1.1 A lower bound for the speed of quantum information

Consider an inertial reference frame centered at the center of the Earth (as depicted in Figure 5.1) that moves with speed $\vec{v}$ with respect to a second inertial reference frame F. Two events A and B occur respectively at locations $\vec{r}_A$ and $\vec{r}_B$ at times t_A and t_B in the Earth reference frame. Let's say that these two events are two single-photon detections with correlations that violate Bell inequalities. If these correlations were caused by an hypothetical influence travelling between the events at a certain speed V_{QI} (that we call *speed of quantum information*), it is the objective of this experiment to find a lower bound for this speed.

For a given privileged frame F, the lower bound on this speed will depend on the orientation of the AB axis and on the alignment of the two events, in the following manner (see Ref. [47] for details on the equation deduction)

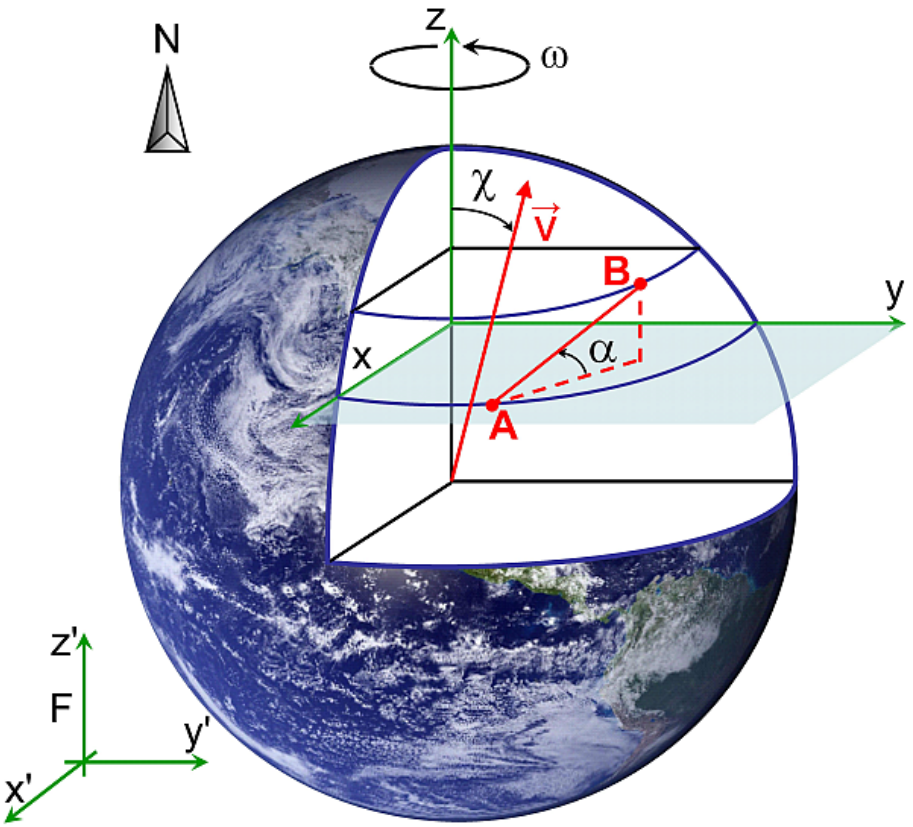

Figure 5.1: The Earth reference frame moves at a speed $\vec{v}$ with respect to a hypothetically privileged reference frame F. The AB axis forms an angle α with the equatorial plane.

$$\left(\frac{V_{QI}}{c}\right)^2 \geq 1 + \frac{(1-\beta^2)(1-\rho^2)}{(\rho+\beta_\parallel)^2} \tag{5.1}$$

where $\beta = \frac{v}{c}$ is the relative speed of the Earth frame in frame F (c being the speed of light), $\beta_\parallel = \frac{v_\parallel}{c}$, is the component of β parallel to the AB axis, and $\rho = \frac{c\, t_{AB}}{r_{AB}}$ quantifies the alignment of the two events in the Earth frame (with $t_{AB} = t_B - t_A$ and $r_{AB} = |\vec{r}_B - \vec{r}_A|$). In the case where $|\rho| < 1$ (which corresponds to spacelike separation), the bound on V_{QI} is then larger than c.

To obtain a high lower bound for V_{QI}, we should upper bound the term $(\rho+\beta_\parallel)^2$ by the smallest possible value, during a period of time T needed to violate the Bell

inequalities (which, in our experiment, will be the integration time of a 2-photon interference fringe). Consider first the simple case where the two events are perfectly simultaneous in the Earth frame ($\rho = 0$), and the AB axis is perfectly aligned in the east-west direction. As the Earth rotates, there will be a moment t_0 when the AB axis is perpendicular to $\vec{v}$, i.e. $\beta_\parallel(t_0) = 0$. During a small time interval around t_0, it is possible to bound $|\beta_\parallel(t)|$ by a small value, and thus obtain a high lower bound for V_{QI}.

It is possible to optimize the alignment ρ for each privileged frame that is about to be tested. This would decrease the upper bound on $(\rho+\beta_\parallel)^2$, while simultaneously increasing the term $(1-\rho^2)$. However, since we want to scan all possible frames, we will not optimize ρ for each frame; instead, we will align the detection events such that $|\rho| \leq \bar{\rho} \ll 1$, where $\bar{\rho}$ is our experimental precision on the alignment ρ. We shall then use the fact that $\frac{1-\rho^2}{(\rho+\beta_\parallel)^2} \geq \frac{1-\bar{\rho}^2}{(\bar{\rho}+|\beta_\parallel|)^2}$, to get the bound

$$\left(\frac{V_{QI}}{c}\right)^2 \geq 1 + \frac{(1-\beta^2)(1-\bar{\rho}^2)}{(\bar{\rho}+|\beta_\parallel|)^2} \tag{5.2}$$

The next step is to find an upper bound for $|\beta_\parallel|$. This magnitude will depend on the angle χ between the speed $\vec{v}$ and the z axis (see Figure 5.1), on the angular velocity of the Earth ω and, in the case where the AB axis is not perfectly aligned with the east-west direction, on the angle α between the AB axis and the equatorial (xy) plane. In this latter case, a period of 24 hours (and not just 12) will be necessary to be able to test all possible privileged referenced frames.

Two possibilities exist for the upper bound on $|\beta_\parallel|$ during a time interval T. Depending whether $\vec{v}$ points close to a pole (i) or not (ii) we obtain (see Ref. [47] for details),

$$(i) \quad |\beta| \left(|\cos\chi \sin\alpha| - |\sin\chi\cos\alpha| \cos\frac{\omega T}{2}\right) \tag{5.3}$$

$$(ii) \quad |\beta| \sqrt{\sin^2\chi\cos^2\alpha - \cos^2\chi\sin^2\alpha}\ \frac{\omega T}{2} \tag{5.4}$$

These bounds, together with equation (5.2), provide the desired lower bound for V_{QI}.

5.2 Experimental setup

The experimental setup used in this experiment is essentially the same as described in chapter 4 and depicted in Figure 4.5, except for the two piezoelectric actuators that play no role in this experiment. The geographical location of the detection stations (at Satigny and Jussy) and the source (in Geneva) is shown in Figure 5.2.

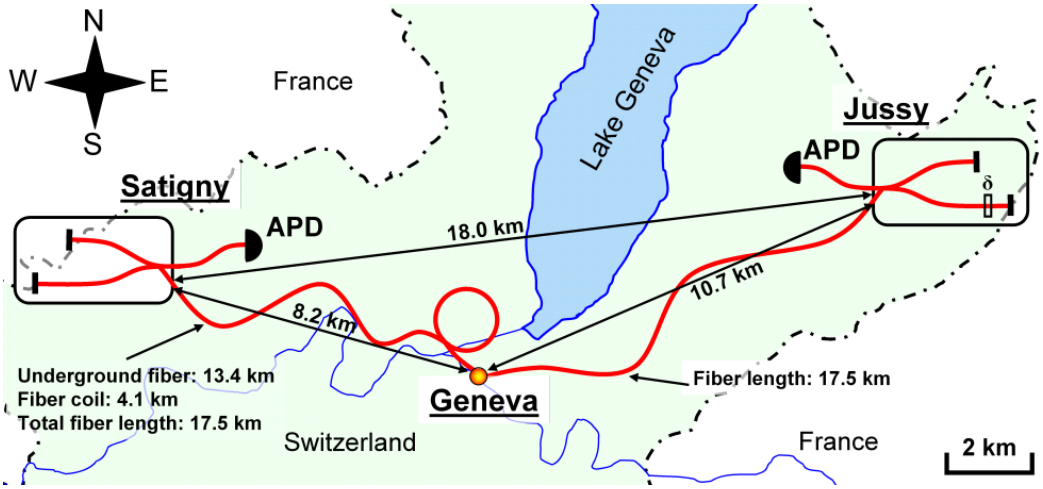

Figure 5.2: Bell experiment setup over 18 km.

To accomplish the condition of simultaneity (in the Earth reference frame), the optical path of each photon must be the same. We can fulfill this condition by adjusting the length of the fibers leading to the detection stations. First, we used an optical time-domain reflectometer (OTDR) [50], to measure the distance from our laboratory to the Swisscom stations at Satigny and Jussy. The fiber leading to Satigny was found to be 4.1 km shorter (13.4 km to Satigny versus 17.5 km to Jussy), so a coiled fiber of this same length was added to this side (it is shown as a loop in Figure 5.2). Additionally, through this same measurement we were able to obtain the loss of light in the fiber. There was around 8 dB of losses on each fiber, mainly due to the connectors linking the several fibers together. Next, we used an optical frequency-domain reflectometer (OFDR) [51] to measure the several short (less than 500 m) fibers that linked the optical elements in the experiment. We managed to reduce the length difference below the uncertainty value associated with the measurement, that

is 1 cm or 49 ps in the arrival time of the photons. Opinions may differ on whether the photons must arrive at the same time at the couplers inside the interferometers or at the photodiodes. To avoid confusion in that matter, the length of the fibers was adjusted with respect to both of these points.

An additional source of uncertainty comes from chromatic dispersion (CD) in the fibers. The fact that the photons are anticorrelated in energy, means that their time delay is opposite to each other, increasing this uncertainty in all cases. This factor added an uncertainty of 319 ps to the arrival times of the photons, bringing the overall uncertainty to $t_{AB} = 323$ ps. This value, together with the direct distance between the detection stations, $r_{AB} = 18.0$ km, allows to estimate the precision of our alignment to a value of $|\rho| \leq \bar{\rho} = 5.4 \cdot 10^{-6} \ll 1$.

5.3 Results and conclusion

To check on the violation of Bell inequalities, the same procedure described in chapter 4 is used here. Coincidence events between the detectors at Satigny and Jussy are continuously recorded while the phase in one of the interferometers is being scanned and the phase of the other is kept stable. Experimental constraints (reaching the end of the scanning range of the interferometer phase and occasional unstabilities of the pump laser) dictate that measurements be taken in several runs, each one lasting several hours (a sample measurement is shown in Figure 5.3).

To check all possible frames, the measurements cover all times of the day. The visibility of the interference fringes remains above the Bell inequalities threshold ($1/\sqrt{2} = 71\%$) in all cases. The length of the visibility fit is equal to one and a half fringes and it was sequentially scanned over all fringes. The visibility values obtained after fitting all the fringes are shown in Figure 5.4.

The violation of Bell inequalities indicates that the correlations are either due to entanglement or the hypothetical influence travels faster than the lower bound that can be determined with this experiment. Using equations 5.2, 5.3 and 5.4, we calculated the value of this lower bound in function of the angle χ and the speed β. In this experiment, the angle between the AB axis and the east-west direction is

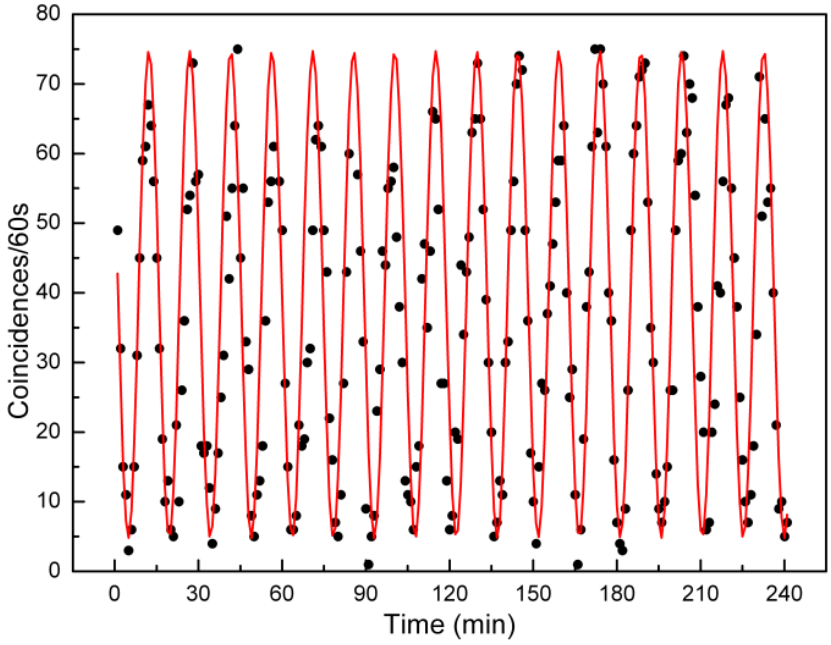

Figure 5.3: Interference fringes measured over 4 hours. The period is 900 s and the net visibility is $V = (94.1 \pm 1.0)\%$. The obtention of long stable periods of fringes like this one was already a remarkable feat for this experiment.

$\alpha = 5.8°$. The period of time needed to observe a Bell violation, which corresponds to the period of one interference fringe, is $T = 360$ s. The resulting graphs are shown in Figure 5.5.

We conclude that if an hypothetical privileged reference frames exists, the speed of the hypothetical influence must be greater than this lower bound. Because of the elevated value of this bound, we think it is unlikely for this influence to exist thus indicating that entanglement occurs instantaneously.

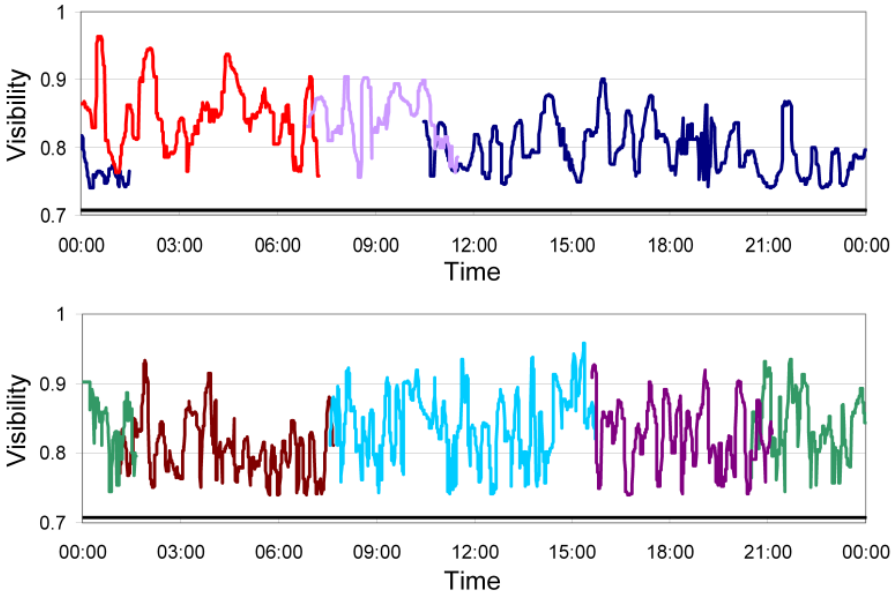

Figure 5.4: We fitted measurements of interference fringes (color lines) covering all the hours of the day twice. The visibility remains above the Bell inequality threshold (black line) at all times.

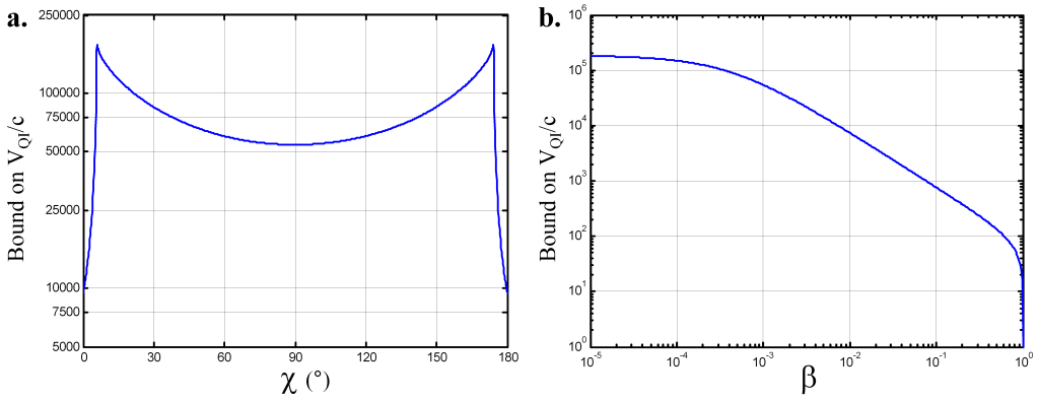

Figure 5.5: Lower bound for the speed of quantum information as a function of (a) the angle χ and $\beta = 10^{-3}$, (b) the speed β and $\chi = 90°$.

Chapter 6

Single-photon entanglement purification

The distribution of entangled states in quantum communication is limited in distance by photon losses in optical fibers. A proposed solution to this problem is the use of quantum repeaters. The idea is to distribute entanglement over short links and then use quantum memories and entanglement swapping to connect several of the links to send entangled states over longer distances. This presents another problem, the deterioration of the entangled states after each operation at which they are submitted. Entanglement purification can be used to recover some of the entanglement that has been lost at the cost of discarding some of the entangled states. The first purification protocols were proposed in 1996 [7, 52]. Entanglement purification can be performed using different forms of entanglement and several protocols have already been tested [53, 54, 25].

In the experiment described in this chapter, we will make use of single-photon entanglement and linear optics elements to obtain purified entangled states [55].

6.1 The purification protocol

Let's say that we have created the entangled state ψ_+. We are using single-photon entanglement so it will be of the form

$$|1\rangle_A|0\rangle_B + |0\rangle_A|1\rangle_B \tag{6.1}$$

where $|0\rangle_{A,B}$ denotes a state with 0 particles (a vacuum state) and $|1\rangle_{A,B}$ a state with 1 particle, in modes A and B.

We send this state to a distant partner but phase errors occur during the transmission and the state that our partner will receive will actually be

$$\rho = F|\psi_+\rangle\langle\psi_+| + (1-F)|\psi_-\rangle\langle\psi_-| \tag{6.2}$$

where ψ_- is an arbitrary state. If $F = 1/2$, no entanglement is left while in the case where $F = 1$, the state is maximally entangled.

We want to purify these phase errors and obtain a state with a higher fidelity. Using the protocol described in [56], we start with two entangled states with fidelity F and we will obtain a purified state with fidelity F_{pur} where $F_{pur} > F$.

The two single-photon entangled states ($\rho_{a_1 b_1}$ with fidelity F_1 and $\rho_{a_2 b_2}$ with fidelity F_2) are distributed to two different partners (Alice and Bob), as shown in Figure 6.1. Each partner performs a local unitary transformation to their respective modes (a_1 and a_2 for Alice, b_1 and b_2 for Bob) using only linear optics elements. The detection of one of the output modes of the transformation (either d_a or d_b) will project the two remaining modes ($\tilde{a}$ and $\tilde{b}$) into a third single-photon entangled state with fidelity

$$\tilde{F} = \frac{F_1 F_2 + F_1/2 + F_2/2}{1 + F_1 F_2 + (1-F_1)(1-F_2)}. \tag{6.3}$$

Assuming indistinguishability of the input modes and for the appropriate transformations, this third state will have become purified. In particular, for errors that reduce the original fidelities a small value ϵ, this protocol divides the errors by half, becoming $\epsilon/2$.

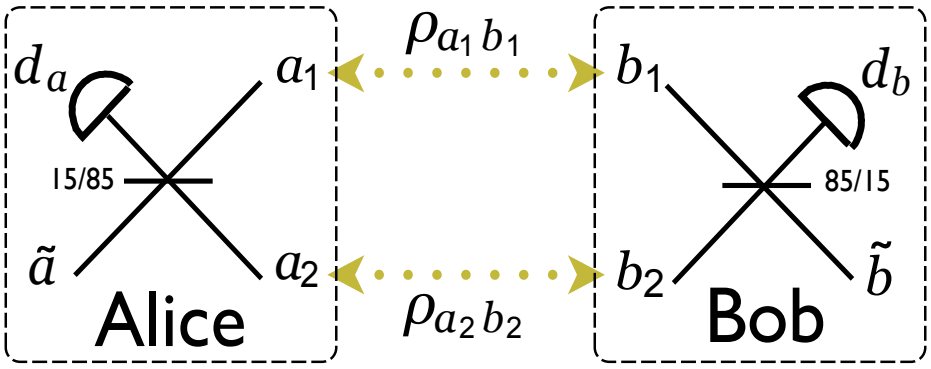

Figure 6.1: Scheme of the purification protocol. Two single-photon entangled states $\rho_{a_1 b_1}$ and $\rho_{a_2 b_2}$ are distributed between two partners (Alice and Bob) who perform a unitary transformation on them. Conditional on the detection of modes d_a (or d_b), modes $\tilde{a}$ and $\tilde{b}$ are projected into a purified entangled state.

6.2 Experimental setup

In this experiment, we use again a non-linear waveguide to create pairs of photons. This time, it is a type-II waveguide so the created photons will have orthogonal polarizations. The waveguide is pumped by a continuous wave laser diode at 780 nm. The wavelength of the laser is locked using the absorption line of the Rubidium (Rb) and a feedback loop.

As shown in Figure 6.2, the photons are separated with a polarizing beamsplitter (PBS) and coupled into optical fibers. Each photon is sent to a 50/50 fiber coupler (BS1 and BS2) where entangled states $\rho_{a_1 b_1}$ and $\rho_{a_2 b_2}$ are created. One mode from each state is sent to Alice, the others are sent to Bob. The unitary transformations are performed by combining the modes with an evanescent wave variable coupler (BS4 and BS5). In the simplest version of the protocol (see [56] for details), the purification efficiency is optimal if the transmission/reflection rates are 85/15 in one coupler and the opposite values in the other. The creation of the purified state $\rho_{\tilde{a}\tilde{b}}$ is conditional on the detection of only one photon on mode d_a (or d_b) by a single-photon detector. Modes $\tilde{a}$ and $\tilde{b}$ are combined at a third 50/50 coupler (BS3) and detected to measure their fidelity.

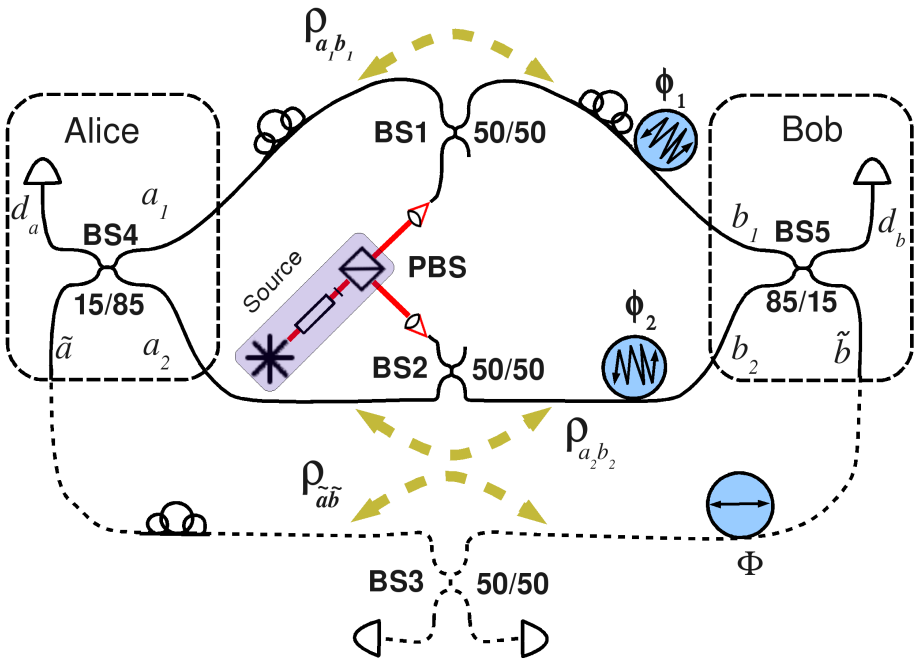

Figure 6.2: Experimental setup for the purification experiment.

6.2.1 Indistinguishability

A critical condition previous to perform entanglement purification is the reduction of the photons distinguishability, which is achieved through the overlap of their spectral, polarization, temporal and transverse spatial modes. If the photons are distinguishable, they will not interfere perfectly, reducing the purification effect. Spectrally, the photons are filtered with a narrowband filter of 1.3 nm of width around a wavelength of 1560 nm. The polarization is controlled with fibered polarization controllers placed along the arms of the interferometer (see Figure 6.2). The temporal overlap is achieved by adjusting the length of the fibers. The transverse spatial overlap is guaranteed by the use of single mode fibers.

The degree of distinguishability of the photons can be measured through the visibility of the Hong-Ou-Mandel dip [57]. This 'dip' appears when the rate of coincidences observed between the outputs of the variable couplers decreases to the noise level due to both photons taking the same path after the coupler. We set the same

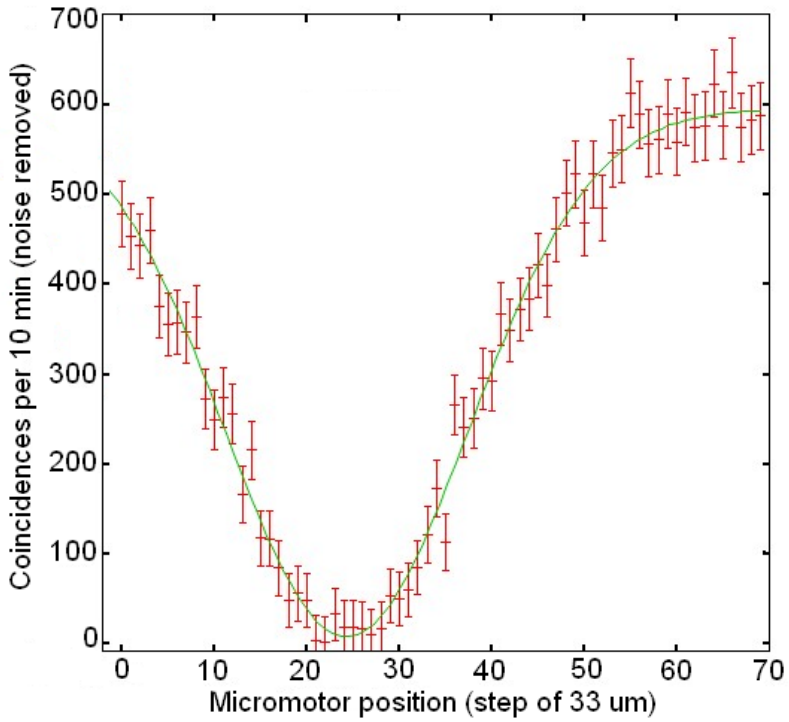

Figure 6.3: HOM dip obtained during the testing phase of the experiment. The achieve indistinguishability, the path length at one of the arms was changed by a micromotor with a step of 33 μm. For each point, coincidences were accumulated for 10 minutes. The visibility is 99.0% and the full width at half maximum is 1056 μm.

transmission ratio on both couplers and measured the coincidence count both when the photons were distinguishable and when they were indistinguishable. To alternate between the two we changed the polarization on one of the arms with the polarization controllers. This method is different from the one used to obtain the dip showed in Figure 6.3 albeit the maximum visibility obtained is the same. We observed a 'dip' with a visibility of $V_{dip} = (C_{max} - C_{min})/C_{max} = (99.0 \pm 0.3)\%$, which is a remarkably high value that satisfies the conditions to perform the purification. The remaining 1.0% is attributed to a non-perfect mode overlap (0.8%) and to double-pair emission (0.2%).

6.2.2 Phase stabilization and noise

The interferometrically sensitive portion of the experimental setup (about 10 m of optical fiber) was placed inside a box to isolate it from the temperature changes in the laboratory. Additionally, the temperature inside the box was controlled and maintained at a stable level. These measures were taken to prevent unwanted phase oscillations of the interferometric phase during the experiment.

To measure the purification of an entangled state we scanned the phase in a controlled way using an annular piezo actuator with a fiber coiled around it. When a voltage is applied to the piezo, its diameter increases due to the piezoelectric effect, stretching the fiber around it. We also introduced artificial noise in a controlled way to reduce the fidelity of the original states to the value where the purification effect is greater, according to the purification protocol [56]. This was done with two additional piezos that vibrated at a frequency higher (≈1 Hz) than the integration time of the measurement (1 point per minute, 25 minutes per fringe). The noise was independently generated for each piezo. The function used to introduce the noise was chosen to reproduce the gaussian phase-noise distribution in a fiber, as observed in real world networks [58].

6.3 Results and conclusion

We first measured the fidelity of the two original states $\rho_{a_1b_1}$ and $\rho_{a_2b_2}$ and obtained values of $F_1 = (97.8\pm0.2)\%$ and $F_2 = (97.7\pm0.2)\%$. Then, we introduced a controlled amount of noise in the fibers that reduced the fidelities to $F_1 = (75.1 \pm 0.8)\%$ and $F_2 = (75.0 \pm 0.7)\%$. These fidelity values were chosen because this is where the purification protocol is more efficient. Finally, we measured the fidelity for the purified state and obtained a value of $\tilde{F} = (79.6 \pm 1.1)\%$. This represents an improvement of 4.5% with respect to the initial fidelities, which is rather high since the theoretical optimal value is 5.7%. The remaining 1.2% is explained mainly by phase fluctuations of modes during the measurement integration times and also due to imperfections in the mode overlap.

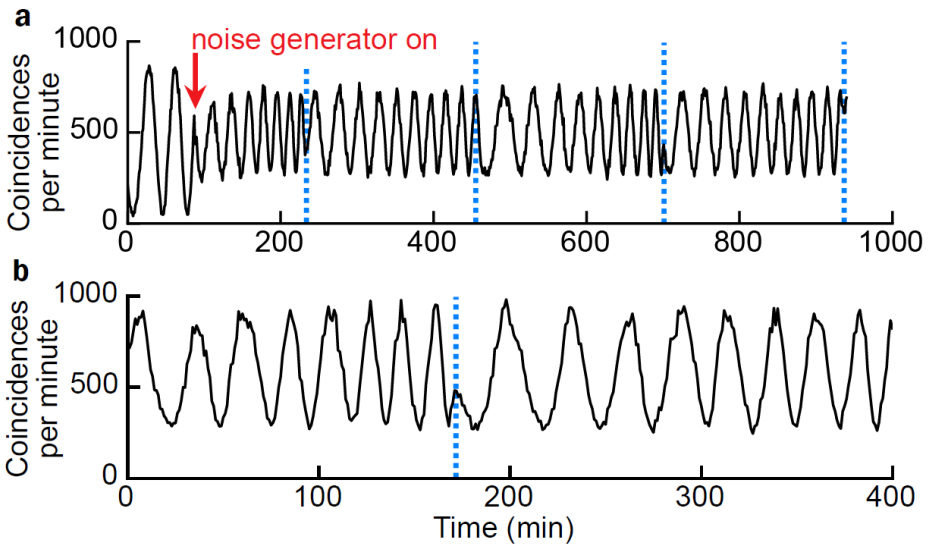

Figure 6.4: Interference fringes obtained while the phase is scanned for a) state $\rho_{a_2b_2}$ and b) state $\rho_{\tilde{a}\tilde{b}}$. We can see how the visibility of the fringes is reduced when the noise is introduced. The blue lines indicate the points where the end of the scanning ramp was reached.

In conclusion, this experiment demonstrates that single-photon entanglement can be purified using only linear optics elements. Regarding the future implementation of this protocol in a quantum repeater, the main challenges would be the use of two independent photon sources and possibly the need for an upgraded phase stabilization system if the fiber lengths are on the order of kilometers.

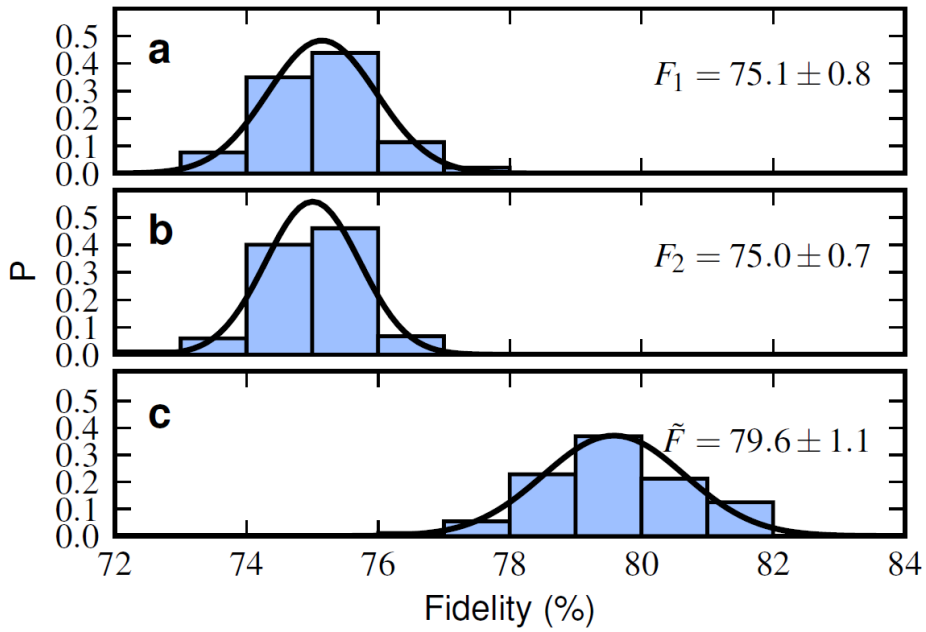

Figure 6.5: Distribution of fidelity values for a) state $\rho_{a_1 b_1}$, b) state $\rho_{a_2 b_2}$ and c) state $\rho_{\tilde{a}\tilde{b}}$. The mean fidelity and standard deviation (σ) are given next to each distribution. The curves are gaussian functions with the same mean and σ as the data.

Chapter 7

Conclusion

During the course of this thesis, we have performed three experiments involving entangled states of photons. The first two are Bell experiments directed to test the nonlocality of quantum correlations. The third is the first test of purification of entanglement that uses only single-photons and linear optics elements.

First, we tested the possibility that a change in the local gravitational field taking place just after the detection events of a spacelike separated Bell experiment, could trigger the collapse of the wavefunction destroying the correlation between the two entangled states. For the first time, a macroscopic mass was used to test if gravitation has an influence over quantum correlations. The verification of this hypothesis lengthened significantly the time of measurement. Consequently, the detection stations had to be situated at distant locations, making this the most separated Bell experiment to date. Even under these strict conditions, a violation of Bell inequalities was observed, acknowledging the nonlocality of entanglement.

We assumed that the change in the mass' position implied an instantaneous change in the surrounding gravitational field. A possible future modification of the experiment would be to measure the change in the gravitational field directly instead of the change in the mass' position. For this purpose, perhaps a measurement similar to that of a Cavendish experiment could be performed. The reason we chose to not carry out this measurement is because with the current technology it is not possible

to perform it in the time required for spacelike separation. It could be feasible, however, if the detection locations were more distant. The limitation in the separation distance comes from the losses in the optical fibers. Another modification involves the use of more massive objects. Note that the time measurement constraints apply here as well.

Second, we tested the idea that an hypothetical influence that propagates faster than the speed of light could travel from the first detection station to the second one and announce the outcome of the detection events. The optical paths of the photons were adjusted to obtain the same travelling time for both photons. Under these conditions, the two events are simultaneous, making it impossible for any signal travelling at a finite speed to reach the other detector in time. The detection locations were chosen to have an almost perfect orientation parallel with the east-west axis of the Earth. This way, all possible reference frames in which this influence can be defined were tested after a measurement period of 24 hours, corresponding to a complete rotation of the Earth. A violation of Bell inequalities was also observed, discarding the existence of this signal if its speed is lower than a bound determined by the experimental uncertainties of our experiment. This bound was calculated to be at least 10000 times the speed of light.

Potential future improvements of this experiment might be directed at obtaining a higher lower bound of the speed of quantum information. To achieve this goal, the first issue would be to obtain a lower uncertainty when determining the precision of the alignment. The main source of uncertainty was the chromatic dispersion in the fibers. Standard telecom fibers have zero dispersion at 1.3-μm. Dispersion-shifted fibers (at 1.5-μm) also exist. To reduce this uncertainty would require either the use of dispersion-shifted fibers or a change in the created photons wavelength to 1310 nm. The first one is unlikely since long distance measurements require the use of the installed optical fiber network. On the other hand, changing the wavelength to 1310 nm implies a higher rate of losses as well as the need for detectors more suited to this wavelength (like Germanium APD's). A different issue is the imperfect east-west orientation of the experiment (non-zero α angle) that reduces the value of the lower bound around low and high χ angles, as it can be seen in Figure 5.5a in chapter 5.

Third, we successfully purified single-photon entangled states using only linear optics elements. Single-photon entanglement purification is more efficient and more simple to realize than purification involving pairs of correlated photons. It is also the most suitable form of purification for many proposals of future quantum repeaters. However, it is heavily dependent on phase oscillations. Single-photon entangled states were created and their entanglement was intentionally reduced through the use of phase noise to simulate real conditions. These states were combined using only fiber couplers and a purified state was obtained. To avoid unwanted phase oscillations, only certain control over the temperature of the optical fibers was required.

The implementation of this protocol in a real world quantum repeater would require the use of two independent sources instead of one. This would probably imply additional work to reduce the distinguishability of photons coming from different sources. For distances on the order of the kilometer or more, the interferometer phase might have to be stabilized with a more precise stabilization system, perhaps using a feedback control like the one used in [59].

To summarize, the bounds obtained in the two Bell experiments make the hypothetical existence of local hidden variables or, alternatively, of a superluminal influence travelling between the detectors, more unlikely than it ever was. In the not so distant future, we can imagine Bell experiments where these hypothesis are further tested at the same time that other loopholes are closed. As for the purification experiment, we know that many quantum repeater protocols use single-photon entanglement. Hopefully, the successful purification of single-photon entangled states brings the practical implementation of a future quantum repeater closer than it has ever been.

Acknowledgements

The work presented in this thesis would not have been possible without the support of several people.

The work presented in chapter 4 was done in collaboration with Augustin Baas. The work presented in chapter 5 was done in collaboration with Cyril Branciard. The source of photon pairs used in the experiments described in chapters 4 and 5 was built by Matthias Leifgen. The work presented in chapter 6 was done in collaboration with Nicolas Sangouard and Olivier Landry.

The projects described in this thesis have been supported by the IST Integrated Project 'Qubit Applications' (QAP) of the European Commission and also by the NCCR Project 'Quantum Photonics' of Switzerland. I thank Swisscom for permitting the use of the installed optical fiber network and the connecting stations for the realization of the experiments.

On a personal level, I would like to thank Professor Nicolas Gisin for giving me the opportunity to do my PhD thesis in the GAP. I also thank Hugo Zbinden for the supervision of this work and for his good suggestions in order to solve experimental problems.

I would like to thank Augustin Baas and Bruno Sanguinetti for always being readily available to answer my questions and for their precious help with the analysis of data. I thank Rob Thew and my labmates Olivier Landry and Jeroen van Houwelingen for their collaboration with the experimental work and for their help whenever I had a question or a doubt.

I specially thank Claudio Barreiro for technical support with the electronics, for his eagerness to help and for interesting discussions on all kind of subjects. I thank

Jean-Daniel Gautier for technical support and help with the electronics related part of the experiments.

I thank Damien Stucki for his help when I started this thesis. Speaking to me only in French during my first months here greatly contributed to learn the language faster.

I thank Patrick, Nino, Enrico, Christoph,... and all the people that work or have worked at the GAP during my stay for the excellent atmosphere that they have contributed to create here in Geneva.

Finally, I especially thank my parents, Pere and Marta, for all the support they gave me when I decided to come to Geneva to do my PhD and also during these four years of thesis.

Bibliography

[1] E. Schrödinger. Discussion of probability relations between separated systems. Proceedings of the Cambridge Philosophical Society **31**, 555-563 (1935); **32**, 446-451 (1936).

[2] A. Einstein, B. Podolsky, and N. Rosen. Can quantum-mechanical description of physical reality be considered complete? Physical Review **47**, 777-780 (1935).

[3] J.S. Bell. On the Einstein-Podolsky-Rosen paradox. Physics **1**, 195200 (1964).

[4] H.-J. Briegel, W. Dür, J.I. Cirac, and P. Zoller. Quantum repeaters: the role of imperfect local operations in quantum communication. Phys. Rev. Lett. **81**, 5932-5935 (1998).

[5] J.-W Pan, D. Bouwmeester, H. Weinfurter, and A. Zeilinger. Experimental entanglement swapping: entangling photons that never interacted. Phys. Rev. Lett. **80**, 3891-3894 (1998).

[6] B. Kraus, W. Tittel, N. Gisin, M. Nilsson, S. Kroll, and J.I. Cirac. Quantum memory for nonstationary light fields based on controlled reversible inhomogeneous broadening. Phys. Rev. A **73** (2), 020302 (2006).

[7] C.H. Bennett, G. Brassard, S. Popescu, B. Schumacher, J.A. Smolin, and W. K. Wootters. Purification of noisy entanglement and faithful teleportation via noisy channels. Phys. Rev. Lett. **76**, 722 (1996).

[8] I. Newton. Philosophiae naturalis principia mathematica. Streater, London (1687).

[9] S.J. Freedman and J.F. Clauser. Experimental test of local hidden-variable theories. Phys. Rev. Lett. **28** (14), 938 (1972).

[10] A. Aspect, J. Dalibard, and G. Roger. Experimental test of Bell's inequalities using time-varying analyzers. Phys. Rev. Lett. **49** (25), 1804-1807 (1982).

[11] A.K. Ekert. Quantum cryptography based on Bell's theorem. Phys. Rev. Lett. **67** (6), 661-663 (1991).

[12] C.H. Bennett, G. Brassard, C. Crépeau, R. Jozsa, A. Peres, and W.K. Wootters. Teleporting an unknown quantum state via dual classical and Einstein-Podolsky-Rosen channels. Phys. Rev. Lett. **70**, 1895 (1993).

[13] R.T. Thew, S. Tanzilli, W.Tittel, H. Zbinden, and N. Gisin. Experimental investigation of the robustness of partially entangled qubits over 11 km. Phys. Rev. A **66**, 062304/1-5 (2002).

[14] J. Brendel, W. Tittel, H. Zbinden, and N. Gisin. Pulsed energy-time entanglement twin photon source for quantum communication. Phys. Rev. Lett. **82**, 2594-2597 (1999).

[15] J. D. Franson. Bell inequality for position and time. Phys. Rev. Lett. **62**, 2205-2208 (1989).

[16] J. Brendel, E. Wohler, and W. Martienssen. Experimental test of Bell inequality for energy and time. Europhys. Lett. **20**, 575 (1992).

[17] P.G. Kwiat, A.M. Steinberg, and R.Y. Chiao. High-visibility interference in a Bell-inequality experiment for energy and time. Phys. Rev. A **47**, 2472-2475 (1993).

[18] S. Tanzilli, H. De Riedmatten, W. Tittel, H. Zbinden, P. Baldi, M. De Micheli, D.B. Ostrowsky, and N. Gisin. Highly efficient photon-pair source using periodically poled lithium niobate waveguide. Elec. Lett. **37**, 2628 (2001).

[19] J.A. Armstrong, N. Bloembergen, J. Ducuing, and P.S. Pershan. Interactions between light waves in a nonlinear dielectric. Phys. Rev. **127**, 1918-1939 (1962).

[20] S.M. Tan, D.F. Walls, and M.J. Collett. Single-particle entanglement. Phys. Rev. Lett. **66**, 252 (1991).

[21] E. Lombardi, F. Sciarrino, S. Popescu, and F. De Martini. Teleportation of a vacuum-one-photon qubit. Phys. Rev. Lett. **88**, 070402 (2002).

[22] B. Hessmo, P. Usachev, H. Heydari, and G. Björk. Experimental demonstration of single-photon nonlocality. Phys. Rev. Lett. **92**, 180401 (2004).

[23] S.B. Papp, K.S. Choi, H. Deng, P. Lougovski, S.J. van Enk, and H.J. Kimble. Characterization of multipartite entanglement for one photon shared among four optical modes. Science **324**, 764-768 (2009).

[24] S.J. van Enk. Single-particle entanglement. Phys. Rev. A **72**, 064306 (2005) and references therein.

[25] K.S. Choi, H. Deng, J. Laurat, and H.J. Kimble. Mapping photonic entanglement into and out of a quantum memory. Nature (London) **452**, 67-71 (2008).

[26] J. F. Clauser, M. A. Horne, A. Shimony, and R. A. Holt. Proposed experiment to test Local Hidden-Variable Theories. Phys. Rev. Lett. **23**, 880 (1969).

[27] W. Tittel, J. Brendel, H. Zbinden, and N. Gisin. Violation of Bell inequalities by photons more than 10 km apart. Phys. Rev. Lett. **81**, 3563 (1998).

[28] A. Aspect. Bell's inequality test: more ideal than ever. Nature **398**, 189 (1999).

[29] M. Lamehi-Rachti, and W. Mittig. Quantum mechanics and hidden variables: a test of Bell's inequality by the measurement of the spin correlation in low-energy proton-proton scattering. Phys. Rev. D **14**, 2543 (1976).

[30] M.A. Rowe, D. Kielpinski, V. Meyer, C.A. Sackett, W.M. Itano, C. Monroe, and D.J. Wineland. Experimental violation of a Bell's inequality with efficient detection. Nature **409**, 791-794 (2001).

[31] D.N. Matsukevich, T. Chanelière, S.D. Jenkins, S.-Y. Lan, T.A.B. Kennedy, and A. Kuzmich. Entanglement of remote atomic qubits. Phys. Rev. Lett. **96**, 030405 (2006).

[32] D.N. Matsukevich, P. Maunz, D.L. Moehring, S. Olmschenk, and C. Monroe. Bell inequality violation with two remote atomic qubits. Phys. Rev. Lett. **100**, 150404 (2008).

[33] A. Aspect, P. Grangier, and G. Roger. Experimental realization of Einstein-Podolsky-Rosen-Bohm *gedankenexperiment*: a new violation of Bell's inequalities. Phys. Rev. Lett. **49** (2), 91-94 (1982).

[34] G. Weihs, T. Jennewein, C. Simon, H. Weinfurter, and A. Zeilinger. Violation of Bell's inequality under strict Einstein locality conditions. Phys. Rev. Lett. **81**, 5039-5043 (1998).

[35] W. Tittel, J. Brendel, H. Zbinden, and N. Gisin. Violation of Bell inequalities by photons more than 10 km apart. Phys. Rev. Lett. **81**, 3563-3566 (1998).

[36] D. Salart, A. Baas, J.A.W. van Houwelingen, N. Gisin, and H. Zbinden. Spacelike separation in a Bell test assuming gravitationally induced collapses. Phys. Rev. Lett. **100**, 220404 (2008).

[37] J. von Neumann. *Mathematische Grundlagen der Quantenmechanik*. Springer, Berlin, (1932) (Mathematical foundations of quantum mechanics. Princeton University Press, 1955).

[38] W.H. Zurek. Decoherence and the transition from quantum to classical. Phys. Today **44**, 36-44 (1991).

[39] H. Everett. 'Relative state' formulation of quantum mechanics. Rev. Mod. Phys. **29**, 454-462 (1957).

[40] R. Penrose. On gravity's role in quantum state reduction. Gen. Rel. Grav. **28**, 581 (1996).

[41] L. Diósi. A universal master equation for the gravitational violation of quantum mechanics. Phys. Lett. A **120**, 377 (1987).

[42] S. Adler. Comments on proposed gravitational modifications of Schrdinger dynamics and their experimental implications. J. Phys. A: Math. Theor. **40**, 755-763 (2007).

[43] A. Kent. A proposed test of the local causality of spacetime. arXiv:gr-qc/0507045v3.

[44] S. Tanzilli, W. Tittel, H. De Riedmatten, H. Zbinden, P. Baldi, M. De Micheli, D.B. Ostrowsky, and N. Gisin. PPLN waveguide for quantum communication. Eur. Phys. J. D **18**, 155-160 (2002).

[45] G. Ribordy, J.-D. Gautier, H. Zbinden, and N. Gisin. Performance of InGaAs/InP avalanche photodiodes as gated-mode photon counters. Appl. Opt. **37** (12), 22722277 (1998).

[46] M. Martinelli, M. J. Marrone, and M. A. Davis. Time reversal for the polarization state in optical systems. J. Mod. Opt. **39**, 451-455 (1992).

[47] D. Salart, A. Baas, C. Branciard, N. Gisin, and H. Zbinden. Testing the speed of 'spooky action at a distance'. Nature **454**, 861-864 (2008) and the related Supplementary Information.

[48] Ph.H. Eberhard. Quantum theory and pictures of reality. ed. W. Schommers, 169-216 (Springer 1989).

[49] V. Scarani, W. Tittel, H. Zbinden, and N. Gisin. The speed of quantum information and the preferred frame: analysis of experimental data. Phys. Lett. A **276**, 1-7 (2000).

[50] F. Scholder, J.-D. Gautier, M. Wegmüller, and N. Gisin. Long-distance OTDR using photon counting and large detection gates at telecom wavelength. Opt. Comm. **213**, 57-61 (2002).

[51] R. Passy, N. Gisin, J.P. von der Weid, and H.H. Gilgen. Experimental and theoretical investigations of coherent OFDR with semiconductor laser sources. J. Lightwave Tech. **12**, 1622-1630 (1994).

[52] D. Deutsch, A. Ekert, R. Jozsa, C. Macchiavello, S. Popescu, and A. Sanpera. Quantum privacy amplification and the security of quantum cryptography over noisy channels. Phys. Rev. Lett. **77**, 2818 (1996).

[53] J.-W. Pan, S. Gasparoni, R. Ursin, G. Weihs, and A. Zeilinger. Experimental entanglement purification of arbitrary unknown states. Nature (London) **423**, 417-422 (2003).

[54] C.-W. Chou, H. de Riedmatten, D. Felinto, S.V. Polyakov, S.J. van Enk, and H.J. Kimble. Measurement-induced entanglement for excitation stored in remote atomic ensembles. Nature (London) **438**, 828-832 (2005); C.-W. Chou, J. Laurat, H. Deng, K.S. Choi, H. de Riedmatten, D. Felinto, and H.J. Kimble. Functional quantum nodes for entanglement distribution over scalable quantum networks. Science **316**, 1316-1320 (2007).

[55] D. Salart, O. Landry, N. Sangouard, N. Gisin, H. Herrmann, B. Sanguinetti, C. Simon, W. Sohler, R.T. Thew, A. Thomas, and H. Zbinden. Purification of single-photon entanglement. Phys. Rev. Lett. **104**, 180504 (2010).

[56] N. Sangouard, C. Simon, T. Coudreau, and N. Gisin. Purification of single-photon entanglement with linear optics. Phys. Rev. A **78**, 050301(R) (2008).

[57] C.K. Hong, Z.Y. Ou, and L. Mandel. Measurement of subpicosecond time intervals between two photons by interference. Phys. Rev. Lett. **59**, 2044 (1987).

[58] J. Minář, H. de Riedmatten, C. Simon, H. Zbinden, and N. Gisin. Phys. Rev. A **77**, 052325 (2008).

[59] S.-B. Cho, and T.-G. Noh. Stabilization of a long-armed fiber-optic single-photon interferometer. Optics Express **17**, 19027-19032 (2009).

Publications

We include the following publications which we have co-authored on subjects described in this thesis:

D. Salart, A. Baas, J.A.W. van Houwelingen, N. Gisin, and H. Zbinden, *Spacelike Separation in a Bell Test Assuming Gravitationally Induced Collapses*, Phys. Rev. Lett. **100**, 220404 (2008).

D. Salart, A. Baas, C. Branciard, N. Gisin, and H. Zbinden, *Testing the speed of spooky action at a distance*, Nature **454**, 861-864 (2008) and the associated Supplementary Information.

D. Salart, O. Landry, N. Sangouard, N. Gisin, H. Herrmann, B. Sanguinetti, C. Simon, W. Sohler, R.T. Thew, A. Thomas, and H. Zbinden, *Purification of Single-Photon Entanglement*, Phys. Rev. Lett. **104**, 180504 (2010).

Spacelike Separation in a Bell Test Assuming Gravitationally Induced Collapses

D. Salart, A. Baas, J. A. W. van Houwelingen, N. Gisin, and H. Zbinden
Group of Applied Physics, University of Geneva, 20, Rue de l'Ecole de Médecine, CH-1211 Geneva 4, Switzerland
(Received 26 March 2008; published 6 June 2008)

We report on a Bell experiment with spacelike separation assuming that the measurement time is related to gravity-induced state reduction. Two energy-time entangled photons are sent through optical fibers and directed into unbalanced interferometers at two receiving stations separated by 18 km. At each station, the detection of a photon triggers the displacement of a macroscopic mass. The timing ensures spacelike separation from the moment a photon enters its interferometer until the mass has moved. Two-photon interference fringes with a visibility of up to 90.5% are obtained, leading to a violation of the Bell inequality.

DOI: 10.1103/PhysRevLett.100.220404 PACS numbers: 03.65.Ud, 42.50.Xa

When is a quantum measurement finished? Quantum theory has no definite answer to this seemingly innocent question and this leads to the quantum measurement problem. Various interpretations of quantum physics suggest opposite views. Some state that a quantum measurement is over as soon as the result is secured in a classical system, though without a precise characterization of classical systems. Decoherence claims that the measurement is finished once the information is in the environment, requiring a clear cut between system and environment and arguments assuring that the system and environment will never recohere. Others claim that it is never over, leading to the many worlds interpretation [1]. Note that none describe how a single event eventually happens. And there are more interpretations and many variations on each theme. In practice this measurement problem has not yet led to experimental tests, though progress in quantum technologies bring us steadily closer to such highly desirable tests [2].

Another possibility, supported among others by Penrose [3] and Diósi [4] (see also the useful review [5]), assumes a connection between quantum measurements and gravity. Intuitively the idea is that the measurement process is finished as soon as space-time gets into a superposition state of significantly different geometries. The latter would be due to superpositions of different configurations of massive objects. Penrose and Diósi independently proposed the same criterion (up to a factor of 2) that relates the time of the collapse (that terminates the measurement) to the gravitational energy of the mass distribution appearing in the superposition. Following Diósi's equation [5], the time of the collapse is given by

$$t_D = \frac{3\hbar V}{2\pi G m^2 d^2}, \tag{1}$$

where V is the volume of the moving object, m is its mass, and d is the distance it has moved.

Hence, according to Eq. (1), a typical measurement in quantum optics is finished once the alternative results would have led to displacements of a sufficiently massive object. This view differs stridently from the one adopted in practice by most quantum opticians. Indeed, the common view in this community is that a quantum measurement is finished as soon as the photons are absorbed by detectors. But such an absorption, even when it triggers an avalanche photodiode and gets registered by a computer, only involves the motion of electrons which are of insufficient mass to satisfy the Penrose-Diósi criterion.

This situation led Kent to observe that actually, according to the Penrose-Diósi criterion, none of the many tests of Bell inequalities that have been performed so far involve spacelike separated events [6] (see Fig. 1). Indeed, in all these tests, no massive object moves, at least not in the microseconds following the photon absorptions by the detectors. But then, none of these Bell tests strictly excludes the possibility that the observed violation of Bell inequalities is due to some hypothetical communication (of a type unknown to today's physics). Given the importance of quantum nonlocality (i.e., violation of Bell inequalities), both for fundamental physics and for quantum information science, we present in this Letter an experiment that closes this loophole.

In our Franson-type test of the Bell inequalities [7], pairs of entangled photons traveling through optical fibers are

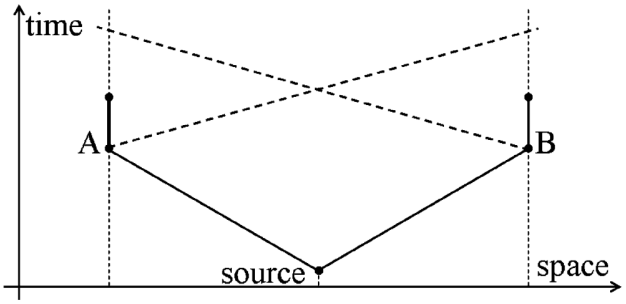

FIG. 1. Space-time diagram of the experiment. When a photon from the source reaches an analyzer (A or B) the measurement process starts. Spacelike separation is achieved when the measurement process at detector A (B) is finished before a light signal traveling from A to B (B to A) arrives at the other detector.

sent to two receiving stations physically separated by 18 km with the source at the center. This distance breaks the record for this kind of experiment [8,9]. At each receiving station, the detected photons trigger the application of a step voltage to a piezoelectric actuator. The actuator is a ceramic-encapsulated PZT (lead zirconate titanate) block of $3 \times 3 \times 2$ mm that weighs 140 mg (PI, PL033). We chose this actuator because it fulfills all the following criteria: it can move a measurable distance in a time of the order of microseconds and it can be triggered to repeat this movement several thousand times per second. Because of the converse piezoelectric effect, the applied voltage expands the actuator and, at the same time, displaces a gold-surfaced mirror measuring $3 \times 2 \times 0.15$ mm and weighing 2 mg that is attached to one of the piezofaces. We used this mirror as the movable mirror of a bulk optical interferometer (see Fig. 2) to confirm the expansion of the piezoactuator (see Fig. 3).

To guarantee the spacelike separation between the detection events, the time that the light needs to travel from one receiving station to the other must be significantly longer than the time needed to perform all the measurement process (t_M). This time includes not only the time of the collapse but also the time between the moment the photons enter their respective analyzer (a 50/50 fiber coupler inside an interferometer), until the moment the mirrors move sufficiently to be certain that the measurement process is finished, according to the Penrose-Diósi hypothesis. The time between the moment the photons enter the analyzer to the moment the step voltage is applied is just 0.1 μs. After the application of the voltage, the piezoactuator starts to expand and displaces the mirror. This produces a change in the phase of the interferometer that is detected by the photodiode. The equivalence between the voltage variation detected by the photodiode and the mirror displacement has been calculated from the wavelength of the laser ($\lambda = 633$ nm) and the phase change produced by the displacement. If we conservatively assume that the phase change takes place in a node of an interference fringe, where the slope between the phase and the intensity is maximum, we will set a lower bound for the displacement distance. Hence, 6 μs after the step voltage is applied to the piezoactuator the voltage has already changed by 0.3 V, for a peak-to-peak maximum of 2.4 V, meaning that the mirror has displaced a distance of at least 12.6 nm. Finally, we find that the time of collapse is $t_D = 1$ μs, using Eq. (1) [10] with $d = 12.6$ nm and taking just the mass and volume of the mirror. The total time is then $t_M = 7.1$ μs, almost 1 order of magnitude shorter than the 60 μs the light needs to cover the 18 km between the receiving stations. Note that taking into account the motion of the piezoactuator itself would even shorten this conservative estimation of t_M.

The scheme of the experimental setup is given in Fig. 4. A cw single mode external cavity diode laser (2.7 mW at 785.2 nm) pumps a periodically poled lithium niobate (PPLN) nonlinear waveguide that creates pairs of photons through the process of spontaneous parametric down-conversion. After the waveguide, a silicon filter (F) blocks all the remaining light at 785.2 nm and the created photon pairs are coupled into an optical fiber. Two circulators and

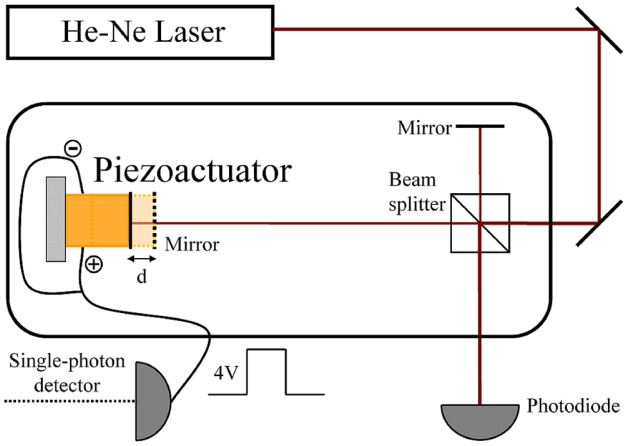

FIG. 2 (color online). Experimental setup of the bulk interferometer used in each receiving station (Satigny and Jussy) to confirm the piezoactuator expansion. Each interferometer is mounted inside a box that isolates it from atmospheric disturbances. The piezoactuator is glued to a fixed support with one mirror attached to its side. Each time a photon is detected by the single-photon detector, a step voltage of 4 V is applied to the piezoactuator, expanding it. When the piezoactuator expands, the laser beam path through the arm with the piezoactuator shortens and the interference produces a variation in the intensity observed by the photodiode.

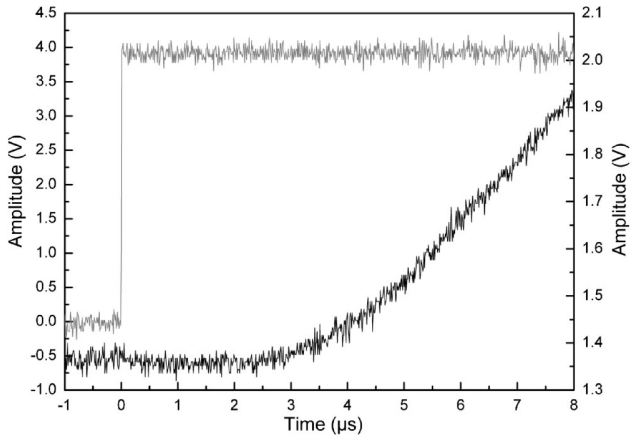

FIG. 3. Step voltage applied on the actuator and the mirror displacement. This measurement confirms the piezoactuator expansion. It was repeated in each receiving station before and after each run of the experiment. Gray line is the step voltage of 4 V (left scale) applied to the piezoactuator. Black line is the distance the mirror has moved represented as the voltage variation (right scale) detected by the photodiode. 6 μs after the voltage is applied, the mirror has already moved by 12.6 nm.

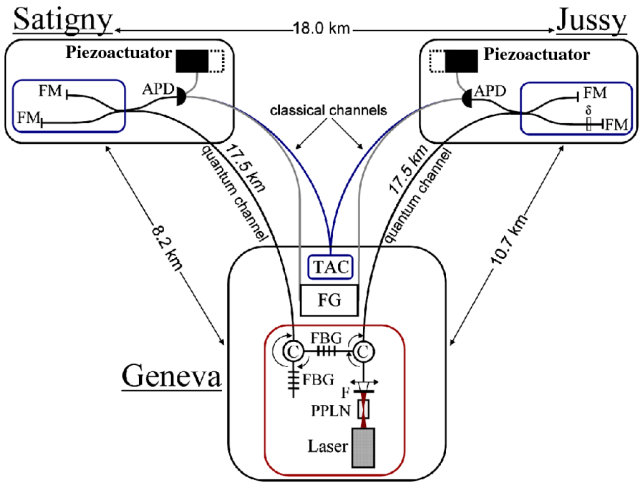

FIG. 4 (color online). Experimental setup. See text for a detailed description.

two fiber Bragg gratings (FBG) separate the pairs according to their wavelength. The first FBG reflects only the photons at 1573.0 nm ($\Delta\lambda = 1.0$ nm) and allows for the rest of the photons to be transmitted, while the second FBG reflects the photons at 1567.8 nm ($\Delta\lambda = 1.0$ nm). The rest of the photons are not transmitted. The photons are sent to their respective receiving stations through standard communication optical fibers. Although the photon's wavelength was chosen to be very close to the third telecommunication window at 1550 nm, there was still around 8 dB of losses in each of the fibers linking the source with the detectors, concentrated mainly at the connectors between different fibers.

The geographical layout of the experiment is such that the source is situated in Geneva and sends the pairs to two receiving stations situated in two villages (Satigny and Jussy) in the Geneva region, at 8.2 and 10.7 km, respectively. The direct distance between them is 18.0 km. At each receiving station, the photons pass through a Michelson interferometer with a long arm and a short arm. The path-length difference is 1.3 ns and is the same in both interferometers. It is also smaller than the coherence length of the pump laser, so an entangled state can be detected when both photons pass through the short (and long) arms. Because the photons are entangled, the probability that pairs of photons choose the same output port can be affected by changing the phase in either interferometer. This will produce interference fringes in the coincidence count when the phase is scanned. To scan the phase, the temperature of one of the interferometers is changed while the other is left stable. To compensate for birefringence effects in the arms of the interferometers (i.e., to stabilize polarization), Faraday mirrors (FM) are used [11].

After passing through the interferometers, the photons are detected by single-photon InGaAs avalanche photodiodes (APDs) (id Quantique, id200). The photodiodes are operated in the gated mode with a repetition frequency of 1 MHz and a gate width of 100 ns. The quantum efficiency is 10% and the dead time is 10 μs. They are triggered in a synchronized way using the same signal sent out from Geneva through other optical fibers. This greatly improves the number of coincidences per unit of time.

Each time the single-photon APDs detect an event, a classical optical signal is sent back to Geneva, where it is detected by a *p-i-n* photodiode. For this, we used the same fibers that were used to send the trigger signal to the APDs. The lasers at both ends of the fibers had different wavelengths (1550 and 1310 nm) and wavelength division multiplexers were used to separate the signals. The detected events are sent to a time-to-amplitude-converter (TAC) that takes one of the signals as start and the other as the stop, measuring the difference in their arrival times. Coincidences in the arrival times between events coming from different detectors indicate that those photons passed either through the short-short or the long-long paths in the interferometers. Using a discriminator with a narrow temporal window, the other two noninterfering possibilities (photons that passed through different arms—short-long or long-short paths) can be discarded.

We monitored the single photon count rates for each detector and the coincidence rate while scanning the phase δ in one of the interferometers. We decrease the temperature of one interferometer slowly and regularly from 40 °C to 21 °C during a period of several hours. The coherence length of the single photons was 2.5 mm, 2 orders of magnitude smaller than the path-length difference in the interferometers (267 mm), so there was no single photon interference, and no phase-dependent variations in the single rates were observed. On the contrary, the coincidence rate showed a sinusoidal oscillation dependent on the phase change in the interferometers. The single count rates were continuously controlled and found constant around 5.0 and 4.1 kHz, including 0.7 and 1.1 kHz of dark counts, for the detectors at Satigny and Jussy, respectively. A discriminator window of 600 ps placed around the coincidence peak gave us an average coincidence rate of 33 coincidences per min.

The Bell inequalities set an upper bound for correlations between particles that can be described by local theories. One of the most frequently used forms is the Clauser-Horne-Shimony-Holt Bell inequality [12], which has a Bell parameter

$$S = |E(d_1, d_2) + E(d_1, d_2') + E(d_1', d_2) - E(d_1', d_2')| \leq 2, \quad (2)$$

where $E(d_1, d_2)$ are the correlation coefficients and d_1, d_2 are values for the phase in the interferometers. Quantum mechanics predicts a maximum value of $S = 2\sqrt{2}$. If the correlation coefficient E is described by a sinusoidal function like $E = V\cos(\delta)$, where δ is the relative phase in the interferometers and V is the visibility, the parameter S

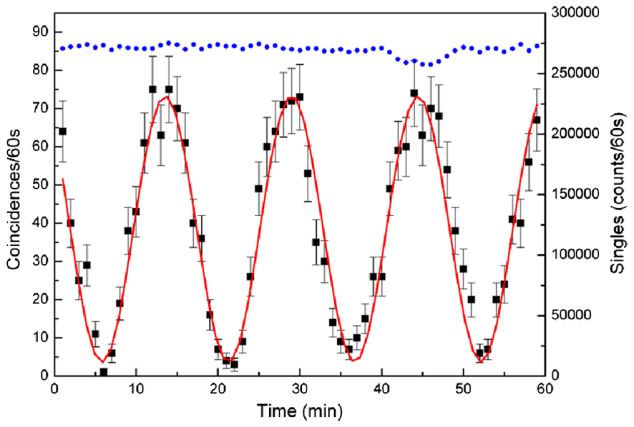

FIG. 5 (color online). Singles (dots) and coincidence counts (squares) per 60 s as a function of time while the phase δ in the Jussy interferometer (see Fig. 4) was being scanned. A best fit with a sinusoidal function yields a visibility of $V_{\text{raw}} = (90.5 \pm 1.5)\%$. Error bars represent the square root of the number of coincidences at each point.

becomes $S = 2\sqrt{2}V$. This implies that if the visibility is $V \geq 1/\sqrt{2}$ the correlations between detected photons is nonlocal.

We are interested in the best visibility value obtained over a period of a few fringes. To obtain an optimal visibility, it is important to have less than 0.1 pairs per time window in order to reduce the probability of having a double pair. The number of photon pairs within the FBG's 1-nm bandwidth was 0.07 pairs per 600 ps time window. The raw data yield a visibility of $V_{\text{raw}} = (90.5 \pm 1.5)\%$ (see Fig. 5) leading to $S_{\text{raw}} = 2.56 \pm 0.04$, surpassing the limit given by the Bell inequalities by 13 standard deviations (σ). We can conclude that the correlations between the photons remain well above the local limit even when the gravitational field is being modified by the displacement of the masses.

Sometimes an avalanche in one of the APDs is set off but without any photon. If such a false detection happens at almost the same time in both APDs or if it happens when one true photon arrives at the other APD, this leads to an accidental coincidence. The number of accidental coincidences will not oscillate with the scannning of the phase but will always remain around the same value, reducing the visibility. The number of accidental coincidences was 2.5 coincidences per min. If we substract the accidentals from the total number of coincidences, the visibility climbs to $V_{\text{net}} = (96.7 \pm 1.4)\%$ leading to $S_{\text{net}} = 2.74 \pm 0.04$, violating the Bell inequalities by 18σ.

In conclusion, we have performed an experimental test of the Bell inequality with spacelike separation large enough to include a hypothetical delay of the quantum state reduction until a macroscopic mass has significantly moved, as advocated by Penrose and Diósi. Indeed, in the reported experiment each detection event triggers the application of a step voltage that expands a piezoactuator and displaces a mirror. The time of collapse of the mirror plus the time it takes to move it is shorter than the time the light needs to travel the distance between the receiving stations. In addition, this distance (18 km) sets a new record for Bell experiments with an independent source located in the middle. Let us emphasize that under the assumption that a quantum measurement is finished only once a gravity-induced state reduction has occurred, none of the many former Bell experiments involve spacelike separation, that is spacelike separation from the time the particles (here photons) enter their measuring apparatuses (here interferometers) until the time the measurement is finished. In this sense, our experiment is the first one with true spacelike separation. The results confirm the nonlocal nature of quantum correlations.

We acknowledge technical support by J.-D. Gautier and C. Barreiro. The access to the telecommunication network was graciously provided by Swisscom. This work was supported by the Swiss NCCR Quantum Photonics and the EU project QAP.

[1] H. Everett, Rev. Mod. Phys. **29**, 454 (1957); B. S. DeWitt, Phys. Today **23**, No. 9, 30 (1970).
[2] I. Percival, Phys. World **10**, 43 (1997); Proc. R. Soc. A **451**, 503 (1995); B. Brezger, L. Hackermüller, S. Uttenthaler, J. Petschinka, M. Arndt, and A. Zeilinger, Phys. Rev. Lett. **88**, 100404 (2002); J.-W. Pan, D. Bouwmeester, M. Daniell, H. Weinfurter, and A. Zeilinger, Nature (London) **403**, 515 (2000); W. Marshall, C. Simon, R. Penrose, and D. Bouwmeester, Phys. Rev. Lett. **91**, 130401 (2003).
[3] R. Penrose, Gen. Relativ. Gravit. **28**, 581 (1996).
[4] L. Diósi, Phys. Lett. A **120**, 377 (1987).
[5] S. Adler, J. Phys. A **40**, 755 (2007).
[6] A. Kent, arXiv:gr-qc/0507045.
[7] J. D. Franson, Phys. Rev. Lett. **62**, 2205 (1989).
[8] A. Aspect, Nature (London) **398**, 189 (1999).
[9] W. Tittel, J. Brendel, H. Zbinden, and N. Gisin, Phys. Rev. Lett. **81**, 3563 (1998).
[10] The Diósi equation gives a value for t_D that is bigger by a factor of 2 with respect to the value given by the Penrose equation.
[11] M. Martinelli, M. J. Marrone, and M. A. Davis, J. Mod. Opt. **39**, 451 (1992).
[12] J. F. Clauser, M. A. Horne, A. Shimony, and R. A. Holt, Phys. Rev. Lett. **23**, 880 (1969).

LETTERS

Testing the speed of 'spooky action at a distance'

Daniel Salart[1], Augustin Baas[1], Cyril Branciard[1], Nicolas Gisin[1] & Hugo Zbinden[1]

Correlations are generally described by one of two mechanisms: either a first event influences a second one by sending information encoded in bosons or other physical carriers, or the correlated events have some common causes in their shared history. Quantum physics predicts an entirely different kind of cause for some correlations, named entanglement. This reveals itself in correlations that violate Bell inequalities (implying that they cannot be described by common causes) between space-like separated events (implying that they cannot be described by classical communication). Many Bell tests have been performed[1], and loopholes related to locality[2–4] and detection[5,6] have been closed in several independent experiments. It is still possible that a first event could influence a second, but the speed of this hypothetical influence (Einstein's 'spooky action at a distance') would need to be defined in some universal privileged reference frame and be greater than the speed of light. Here we put stringent experimental bounds on the speed of all such hypothetical influences. We performed a Bell test over more than 24 hours between two villages separated by 18 km and approximately east–west oriented, with the source located precisely in the middle. We continuously observed two-photon interferences well above the Bell inequality threshold. Taking advantage of the Earth's rotation, the configuration of our experiment allowed us to determine, for any hypothetically privileged frame, a lower bound for the speed of the influence. For example, if such a privileged reference frame exists and is such that the Earth's speed in this frame is less than 10^{-3} times that of the speed of light, then the speed of the influence would have to exceed that of light by at least four orders of magnitude.

According to quantum theory, quantum correlations violating Bell inequalities simply happen, somehow from outside space-time, in the sense that there is no space-time explanation for their occurrence: there is no event here that somehow influences another distant event there. Yet such a description of correlations, which is radically different from all those found in any other part of science, should be thoroughly tested.

In 1989, Eberhard[7] realized that the existence of a hypothetically privileged reference frame can be experimentally tested for. The idea is that the speed of this influence, although greater than the speed of light, is finite. Hence, if the events are simultaneous in the hypothetically privileged frame, then the signal does not arrive on time and no violation of Bell inequalities should be observed. Note that if the events are simultaneous in some reference frame, then they are also simultaneous with respect to any reference frame moving in a direction perpendicular to the line joining the two events. Accordingly, Eberhard proposed (Ph. H. Eberhard, personal communication) to perform a Bell test over a long distance oriented east–west, over a period of 12 hours (ref. 8). If the events were simultaneous in the Earth's reference frame, then they would also be simultaneous with respect to all frames moving in the plane perpendicular to the east–west axis, and in 12 hours all possible hypothetically privileged frames would be scanned. An intriguing alternative, that we will not follow here, is to speculate that there is a tachyonic field[9] that couples specifically to entangled particles.

Bohm's[10] pilot-wave model of quantum mechanics is an example of a theory containing an explicit spooky action at a distance, which requires the assumption that there is a universally privileged frame[11]. Also, if the spooky action at a distance propagates at finite speed, then an experiment like the one presented below could possibly falsify the pilot-wave model[12]. Reference 12 stresses that the existence of a universally privileged frame would not contradict relativity.

By 2000, a Bell experiment along the lines presented above had already been analysed[8,13,14]. However, the analysis concerned only two hypothetically privileged reference frames. The first frame was defined by the ~2.7 K cosmic microwave background radiation. The second frame analysed was the 'Swiss Alps reference frame', that is, not a universal frame but merely the frame defined by the massive environment of the experiment. The assumption that the privileged frame depends on the experiment's environment leads naturally to the issue of situations in which the massive environments on both sides of the experiment differ, and this was the main subject of the experiment in 2000 (refs 13, 14). In both of these analyses, the hypothetical superluminal influence was termed the speed of quantum information to stress that it is not classical signalling. We shall use this terminology, but we emphasize that this is only the speed of a hypothetical influence and that our result casts very serious doubts on its existence. For views on the speed of quantum information, see ref. 15.

Before presenting our experiment and results, let us clarify the principle of our measurements and how to obtain bounds on this speed of quantum information in any reference frame.

In an inertial reference frame centred on the Earth, two events A and B (in our experiment two single-photon detections) respectively occur at positions $\mathbf{r}_A$ and $\mathbf{r}_B$ at times t_A and t_B. Let us consider another inertial reference frame F, the hypothetically privileged frame, relative to which the Earth frame moves with a velocity $\mathbf{v}$ (Fig. 1). When correlations violating a Bell inequality are observed, the speed of quantum information V_{QI} in frame F that could cause the correlation is bounded from below as follows:

$$V_{QI} \geq \frac{\left\|\mathbf{r}'_B - \mathbf{r}'_A\right\|}{\left|t'_B - t'_A\right|}$$

where $(\mathbf{r}'_A, t'_A)$ and $(\mathbf{r}'_B, t'_B)$ are respectively the coordinates of events A and B in frame F, obtained from $(\mathbf{r}_A, t_A)$ and $(\mathbf{r}_B, t_B)$ by Lorentz transformation. After simplification, we obtain

$$\left(\frac{V_{QI}}{c}\right)^2 \geq 1 + \frac{(1-\beta^2)(1-\rho^2)}{(\rho+\beta_{||})^2} \quad (1)$$

where $\beta = v/c$ is the speed ($v = ||\mathbf{v}||$) of the Earth frame in frame F relative to the speed of light (c); $\beta_{||} = v_{||}/c$, with $v_{||}$ the component of $\mathbf{v}$ parallel to the A–B axis; and $\rho = ct_{AB}/r_{AB}$ quantifies the alignment of the two events in the Earth frame, with $t_{AB} = t_B - t_A$ and $r_{AB} = ||\mathbf{r}_B - \mathbf{r}_A||$. In the following, we will consider space-like separated

[1]Group of Applied Physics, University of Geneva, 20 Rue de l'Ecole de Médecine, CH-1211 Geneva 4, Switzerland.

events, for which $|\rho| < 1$: the bound on V_{QI} in equation (1) will then be larger than c. For a given privileged frame F, this bound depends on the orientation of the A–B axis through $\beta_{||}$ and on the alignment ρ. To obtain a good lower bound for V_{QI}, we should bound the term $(\rho + \beta_{||})^2$ from above by the smallest possible value, during a period of time T needed to observe a Bell violation (which, in our experiment, will be the integration time of a two-photon interference fringe).

To gain some intuition, we first consider the simple case in which $\rho = 0$ (the two events are perfectly simultaneous in the Earth frame) and the A–B axis is perfectly aligned in the east–west direction. Then, when the Earth rotates, there will be a moment t_0 when the east–west direction is perpendicular to **v**, that is, $\beta_{||}(t_0) = 0$. During a small time interval around t_0, we can bound $|\beta_{||}(t)|$ by a small value, and thus obtain a high lower bound for V_{QI}.

In principle, the alignment ρ could be optimized for each privileged frame that we wish to test, so as to decrease the bound that can be put on $(\rho + \beta_{||})^2$ during the time interval T (and increase the term $(1 - \rho^2)$ at the same time). In our experiment, however, because we want to scan all possible frames, we do not optimize ρ for each frame; instead, we align the detection events such that $|\rho| \leq \bar{\rho} \ll 1$, where $\bar{\rho}$ is our experimental precision on the alignment ρ. We then use the fact that $(1-\rho^2)/(\rho+\beta_{||})^2 \geq (1-\bar{\rho}^2)/(\bar{\rho}+|\beta_{||}|)^2$ to get the following bound:

$$\left(\frac{V_{QI}}{c}\right)^2 \geq 1 + \frac{(1-\beta^2)(1-\bar{\rho}^2)}{(\bar{\rho}+|\beta_{||}|)^2} \qquad (2)$$

The problem reduces to bounding $|\beta_{||}|$ directly.

In the configuration of our experiment, the A–B axis is almost, but not perfectly, oriented along the east–west direction. Consequently, the component $\beta_{||}(t)$ has a 24-hour period, and geometric considerations show that it can be written as (see the Supplementary Information)

$$\beta_{||}(t) = \beta \cos\chi \sin\alpha + \beta \sin\chi \cos\alpha \cos\omega t$$

where χ is the zenith angle of **v**, α is the angle between the A–B axis and the equatorial x–y plane (Fig. 1), and ω is the angular velocity of the Earth.

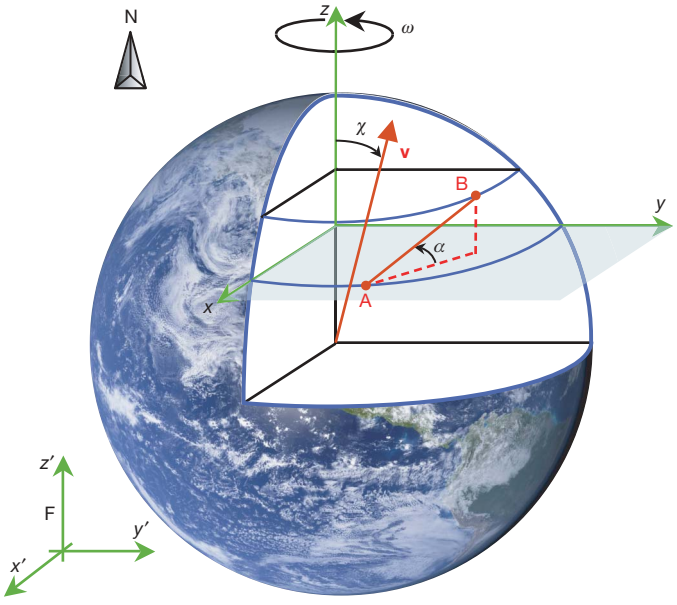

Figure 1 | Reference frames. The Earth frame moves with respect to a hypothetically privileged reference frame F at a speed **v**. The zenith angle χ between **v** and the z axis can have values between 0° and 180°. The A–B axis forms an angle α with the equatorial (x–y) plane. ω, angular velocity of the Earth.

As we show in the Supplementary Information, in order to bound $|\beta_{||}|$ from above during a period of time T, we can consider two cases: one in which **v** does not point close to a pole ($C_T|\tan\chi| > |\tan\alpha|$), and one in which it does ($C_T|\tan\chi| \leq |\tan\alpha|$). Here $C_T = \cos^2(\omega T/4)$, which ~ 1 when ωT is small. There exists a time interval of length T during which $|\beta_{||}(t)|$ is bounded from above by

$$|\beta|\sqrt{\sin^2\chi\cos^2\alpha - \cos^2\chi\sin^2\alpha}\,\frac{\omega T}{2}$$

in the first case and by

$$|\beta|\left(|\cos\chi\sin\alpha| - |\sin\chi\cos\alpha|\cos\frac{\omega T}{2}\right)$$

in the second case. These bounds, together with equation (2), provide the desired lower bound for V_{QI}.

We now describe our experiment. In essence it is a large Franson interferometer[16]. A source situated in our laboratory in Geneva emits entangled photon pairs using the standard parametric down-conversion process in a nonlinear crystal (here a continuous-wave laser pumps a waveguide in a periodically poled lithium niobate crystal)[17]. Using fibre Bragg gratings and optical circulators, each pair is deterministically split and one photon is sent through the Swisscom fibre optic network to Satigny, a village west of Geneva, and the other photon is sent to Jussy, a village east of Geneva. The two receiving stations, located in those two villages, are separated by a direct distance of 18.0 km (Fig. 2). We use energy–time entanglement, a form of entanglement well suited to quantum communication in standard telecommunications fibres[18]. At each receiving station, the photons pass through identically unbalanced fibre-optic Michelson interferometers. The imbalance ($\sim$25 cm) is larger than the single-photon coherence length ($\sim$2.5 mm), meaning that any single-photon interference is avoided, but is much smaller than the pump laser coherence length (>20 m). Accordingly, when a photon pair is detected simultaneously in Satigny and Jussy, there is no information about which path—the long arm or the short arm—the photons took in their interferometers. But because the photons were also emitted simultaneously, they must both have taken the same long or short path. This indistinguishability leads, as always in quantum physics, to interference between the long–long and short–short paths. Continuously scanning the phase in one interferometer (at Jussy), while keeping the other one stable, produces a sinusoidal oscillation of the correlation between the photon detections at Satigny and Jussy (Fig. 3). The phases were controlled by the temperature of the fibre-based interferometers.

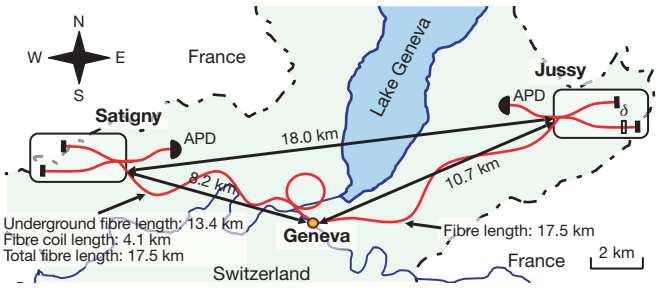

Figure 2 | Experimental setup. The source sends pairs of photons from Geneva to two receiving stations through the Swisscom fibre-optic network. The stations are situated in two villages, Satigny and Jussy, that are respectively 8.2 and 10.7 km from Geneva. The direct distance between them is 18.0 km. At each receiving station, the photons pass through identically unbalanced Michelson interferometers and are detected by a single-photon InGaAs avalanche photodiode (APD) (id201, id Quantique). The length of the fibre going to Jussy is 17.5 km. The fibre going to Satigny is only 13.4 km long, so we added a fibre coil of 4.1 km (represented as a loop) to equalize the lengths of the fibres. Having fibres with the same length allows us to satisfy the condition of good alignment ($\rho \ll 1$). δ indicates the scanning of the phase of the interferometer at Jussy.

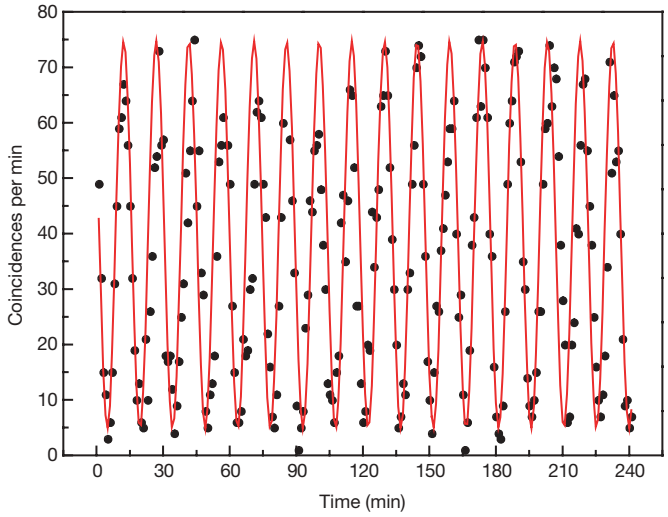

Figure 3 | Interference fringes. Interference fringes with a period $T = 900$ s obtained during a 4-hour measurement, fitted with a sinusoidal function yielding a visibility of 87.6% ± 1.1%. If we subtract the accidental coincidences, the (net) visibility climbs to 94.1% ± 1.0%. This result is significant because the period of the interference fringes remains stable for a very long time, which allows us to fit the entire measurement with a continuous fit and obtain a high visibility value.

Interference fringes were recorded in many runs, which usually lasted several hours (up to 15 hours for the longest run (see Fig. 4)). By juxtaposing several of these measurement runs obtained over several weeks, we covered a 24-hour period with interference fringe periods of $T = 360$ s with visibilities well above the threshold $(1/\sqrt{2})$ set by the Clauser–Horne–Shimony–Holt Bell inequality[19]. The visibility is large enough to exclude any common-cause explanation. The correlations are thus due either to entanglement, as predicted by quantum physics, or to some hypothetical spooky action at a distance whose speed we wish to bound from below. Because long measurements of fringes with short fringe periods T are difficult to fit continuously, we fitted the data over a time window corresponding to one-and-a-half fringes and scanned this time window, as explained in the Supplementary information.

The violation of the Bell inequality at all times of day makes it possible to calculate the lower bound for the speed of quantum information in any reference frame. This bound depends on the precision of the alignment in the actual experiment; see equation (2). We wished to have a good alignment ($\rho \ll 1$), so the difference in the arrival times of the single photons t_{AB} was minimized.

First, the length of each fibre between the source and the single-photon detectors was measured. The long fibres (several kilometres in length) were measured using a single-photon optical time-domain reflectometer[20] and the short fibres (less than 500 m in length) were measured using an optical frequency-domain reflectometer[21]. The fibre on the Satigny side was found to be shorter than the other by 4.1 km. We added a fibre coil to the short side (represented as a loop in Fig. 2), reducing this difference to below 1 cm with an uncertainty of 1 cm, which corresponds to a light travel time of 49 ps. To remove any doubt about where exactly the measurement took place, we adjusted the lengths of the fibres from the source to the fibre couplers inside each interferometer and also to the photodiodes (where the photons are detected). Hence, the configuration was totally symmetric.

Next, we considered the chromatic dispersion in the fibres. Chromatic dispersion added an uncertainty in the arrival times, and because the entangled photons were anticorrelated in energy, their time delays were always opposite to each other, which always increased this uncertainty. Chromatic dispersion was measured to be 18.2 ps nm^{-1} km^{-1} using a chromatic dispersion analyser[22]. For a spectral half-width of $\Delta\lambda = 0.5$ nm and twice the distance of 17.5 km, this is equivalent to a 319-ps uncertainty. Thus, the overall uncertainty in the relative lengths of the fibres was, when expressed in light travel time, $t_{AB} = 323$ ps. This, together with the direct distance between the receivers, $r_{AB} = 18.0$ km, allowed us to estimate the precision of our alignment: $|\rho| \leq \bar{\rho} = 5.4 \times 10^{-6} \ll 1$.

Last, we used equation (2) to calculate a lower bound for V_{QI}. We used the value of $\bar{\rho}$ just calculated, the period of time $T = 360$ s needed to observe a Bell violation (corresponding to the interference fringe period), and the angle formed by the axis between the two receiving stations (the A–B axis) and the equatorial (x–y) plane, $\alpha = 5.8°$. The results are shown in Fig. 5, for certain hypothetically privileged frames. In Fig. 5a, we scan all possible directions χ, but set the Earth's relative

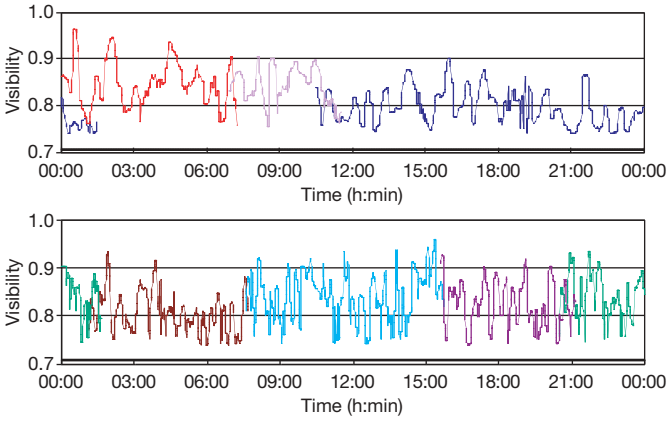

Figure 4 | Visibility fits. Visibility fits for several uninterrupted runs obtained at different times of the day. Together these runs cover each moment of the day at least twice. The limitations on the lengths of these measurements were due to the end of the cooling ramp and small instabilities in the set-up that produced short interruptions in the scan. Visibility values remain above the threshold value of $1/\sqrt{2}$ (black line) set by the Clauser–Horne–Shimony–Holt Bell inequality at all times.

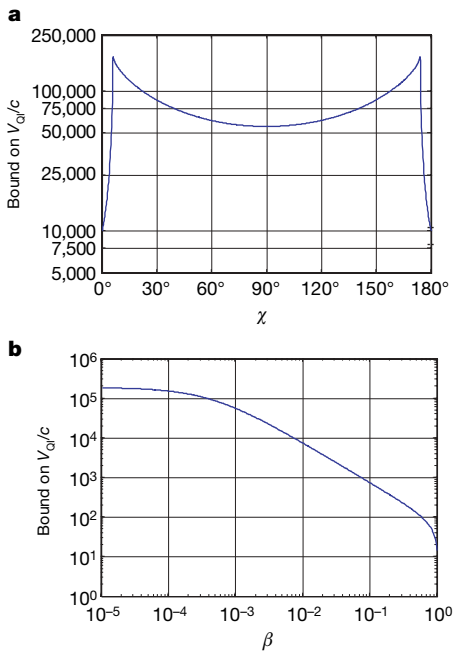

Figure 5 | Lower bounds for the speed of quantum information. **a**, Bound obtained for V_{QI}/c as a function of the angle χ, for $\beta = 10^{-3}$. For $\chi \lesssim \alpha$ or $\chi \gtrsim 180° - \alpha$, the bound is obtained by considering the second case discussed in the text, whereas for $\alpha \lesssim \chi \lesssim 180° - \alpha$, the bound is obtained by considering the first case. The bound at $\chi = 90°$ is $V_{QI} \geq 54{,}000c$. **b**, Bound obtained for V_{QI}/c as a function of the speed β, for $\chi = 90°$. As β tends to zero, our bound on V_{QI}/c tends to $1/\bar{\rho}$.

speed at $\beta = 10^{-3}$. A lower bound for V_{QI} greater than 10,000 times the speed of light is found in any such reference frame. The imperfect east–west orientation ($\alpha \neq 0$) is responsible for the minimum values of the bound at angles χ near 0° and 180°. For smaller Earth speeds, the bound on V_{QI} is even larger. However, if β is very large, then the corresponding bound on V_{QI} is less stringent. To illustrate this, in Fig. 5b we set $\chi = 90^\circ$, that is, with $\mathbf{v}$ in the equatorial plane, and scan the velocity β. Indeed, for $\beta \approx 1$, the bound drops rapidly. Recall, however, that for large values of β we could in principle optimize the alignment ρ in the experiment to get a better bound on V_{QI}. For small values of β, our bound is limited by the inverse of our precision of alignment $\bar{\rho}$.

In conclusion, we performed a Bell experiment using entangled photons between two villages separated by 18 km and approximately east–west oriented, with the source located precisely in the middle. The rotation of the Earth allowed us to test all possible hypothetically privileged frames over a period of 24 hours. Two-photon interference fringes with visibilities well above the threshold set by the Bell inequality were observed at all times of day. From these observations we conclude that the nonlocal correlations observed here and in previous experiments[1] are indeed truly nonlocal. To maintain an explanation based on spooky action at a distance we would have to assume that the spooky action propagates at speeds even greater than the bounds obtained in our experiment.

Received 2 April; accepted 30 May 2008.

1. Aspect, A. Bell's inequality test: more ideal than ever. *Nature* **398,** 189–190 (1999).
2. Aspect, A. *et al.* Experimental realization of Einstein-Podolsky-Rosen-Bohm Gedankenexperiment: A new violation of Bell's inequalities. *Phys. Rev. Lett.* **49,** 91–94 (1982).
3. Tittel, W., Brendel, J., Zbinden, H. & Gisin, N. Violation of Bell inequalities by photons more than 10 km apart. *Phys. Rev. Lett.* **81,** 3563–3566 (1998).
4. Weihs, G., Jennewein, T., Simon, C., Weinfurter, H. & Zeilinger, A. Violation of Bell's inequality under strict Einstein locality conditions. *Phys. Rev. Lett.* **81,** 5039–5043 (1998).
5. Rowe, M. A. *et al.* Experimental violation of a Bell's inequality with efficient detection. *Nature* **409,** 791–794 (2001).
6. Matsukevich, D. N. *et al.* Bell inequality violation with two remote atomic qubits. *Phys. Rev. Lett.* **100,** 150404 (2008).
7. Eberhard, PhH *Quantum Theory and Pictures of Reality* (ed. Schommers, W.) 169–216 (Springer, Berlin, 1989).
8. Scarani, V. *et al.* The speed of quantum information and the preferred frame: analysis of experimental data. *Phys. Lett. A* **276,** 1–7 (2000).
9. Feinberg, G. Possibility of faster-than-light particles. *Phys. Rev.* **159,** 1089–1105 (1967).
10. Bohm, D. A suggested interpretation of the quantum theory in terms of "hidden" variables I. *Phys. Rev.* **85,** 166–179 (1952).
11. Bohm, D. A suggested interpretation of the quantum theory in terms of "hidden" variables II. *Phys. Rev.* **85,** 180–193 (1952).
12. Bohm, D. & Hiley, B. J. *The Undivided Universe* 293 (Routledge, London, 1993).
13. Gisin, N., Scarini, V., Tittel, W. & Zbinden, H. Optical tests of quantum nonlocality: from EPR-Bell tests towards experiments with moving observers. *Annal. Phys.* **9,** 831–841 (2000).
14. Zbinden, H. *et al.* Experimental test of nonlocal quantum correlation in relativistic configurations. *Phys. Rev. A* **63,** 022111 (2001).
15. Garisto, R. What is the speed of quantum information? Preprint at ⟨http://arxiv.org/abs/quant-ph/0212078⟩ (2002).
16. Franson, J. D. Bell inequality for position and time. *Phys. Rev. Lett.* **62,** 2205–2208 (1989).
17. Tanzilli, S. *et al.* PPLN waveguide for quantum communication. *Eur. Phys. J. D* **18,** 155–160 (2002).
18. Thew, R. *et al.* Experimental investigation of the robustness of partially entangled qubits over 11 km. *Phys. Rev. A* **66,** 062304 (2002).
19. Clauser, J. F., Horne, M. A., Shimony, A. & Holt, R. A. Proposed experiment to test local hidden-variable theories. *Phys. Rev. Lett.* **23,** 880–884 (1969).
20. Scholder, F., Gautier, J.-D., Wegmüller, M. & Gisin, N. Long-distance OTDR using photon counting and large detection gates at telecom wavelength. *Opt. Commun.* **213,** 57–61 (2002).
21. Passy, R. *et al.* Experimental and theoretical investigations of coherent OFDR with semiconductor laser sources. *J. Lightwave Technol.* **12,** 1622–1630 (1994).
22. Brendel, J., Gisin, N. & Zbinden, H. in *Proc. 5th Opt. Fiber Measurement Conf.* (eds Boisrobert, Ch. & Tanguy, E.) 12–17 (Université de Nantes, Nantes, 1999).

Supplementary Information is linked to the online version of the paper at www.nature.com/nature.

Acknowledgements We acknowledge technical support by J.-D. Gautier and C. Barreiro. The access to the telecommunications network was provided by Swisscom. This work was supported by the Swiss NCCR Quantum Photonics and the European Union project QAP. The image of the Earth in Fig. 1 is a NASA Goddard Space Flight Center Image by R. Stöckli.

Author Information Reprints and permissions information is available at www.nature.com/reprints. Correspondence and requests for materials should be addressed to D.S. (daniel.salart@physics.unige.ch).

Testing the speed of spooky action at a distance

Daniel Salart[1], Augustin Baas[1], Cyril Branciard[1], Nicolas Gisin[1] & Hugo Zbinden[1]

Supplementary Figures and Legends

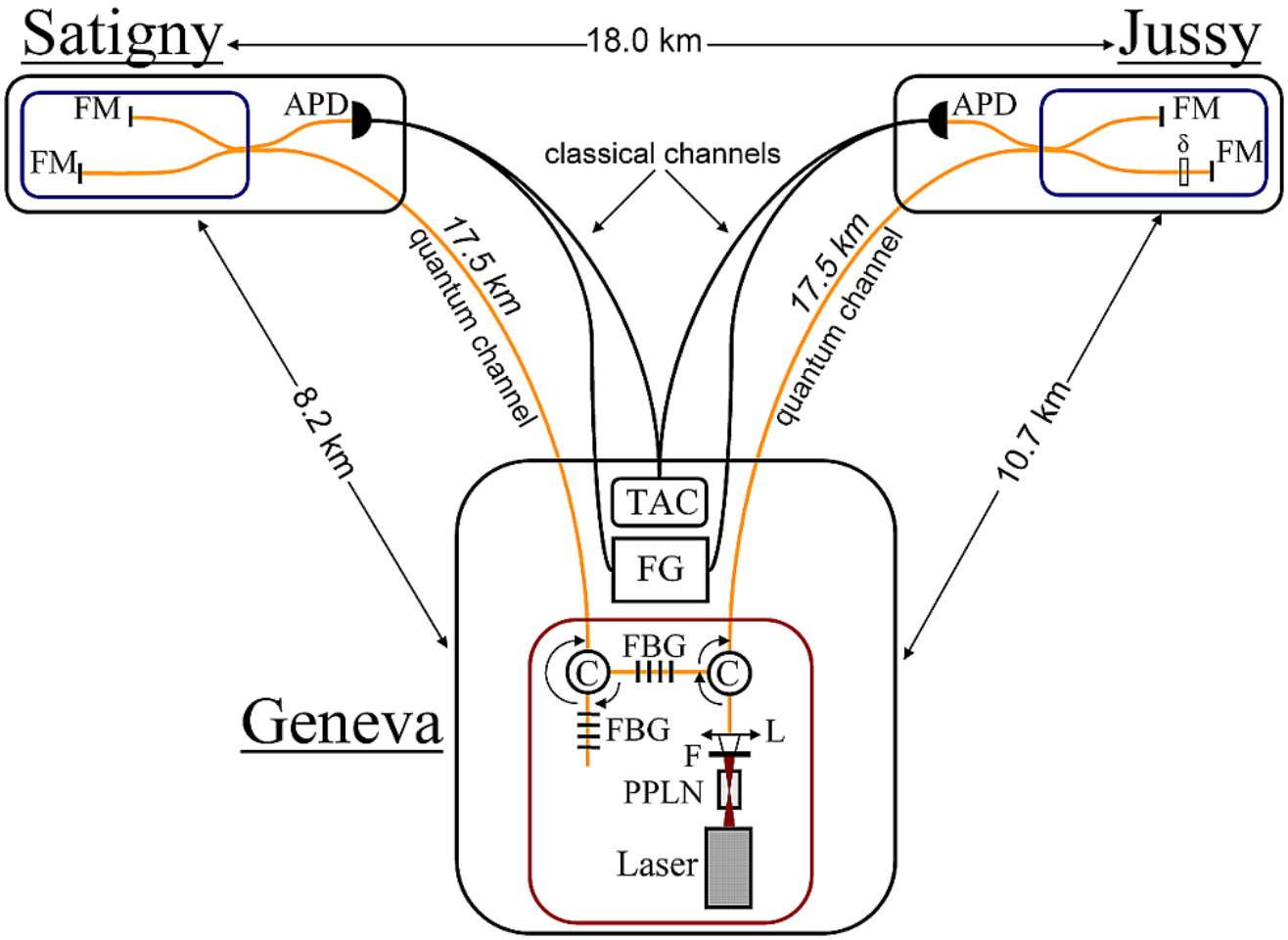

Supplementary Figure 1 | Experimental setup. A cw laser pumps a nonlinear waveguide creating pairs of entangled photons. Each photon is sent to a receiving station located several km away through installed optical fibers. After travelling through a Michelson interferometer with arms of different length, each photon is detected by an avalanche photodiode. Detection events are continuously monitored in search for coincidences in their arrival times.

[1]Group of Applied Physics, University of Geneva, 20, Rue de l'Ecole de Médecine, CH-1211 Geneva 4, Switzerland

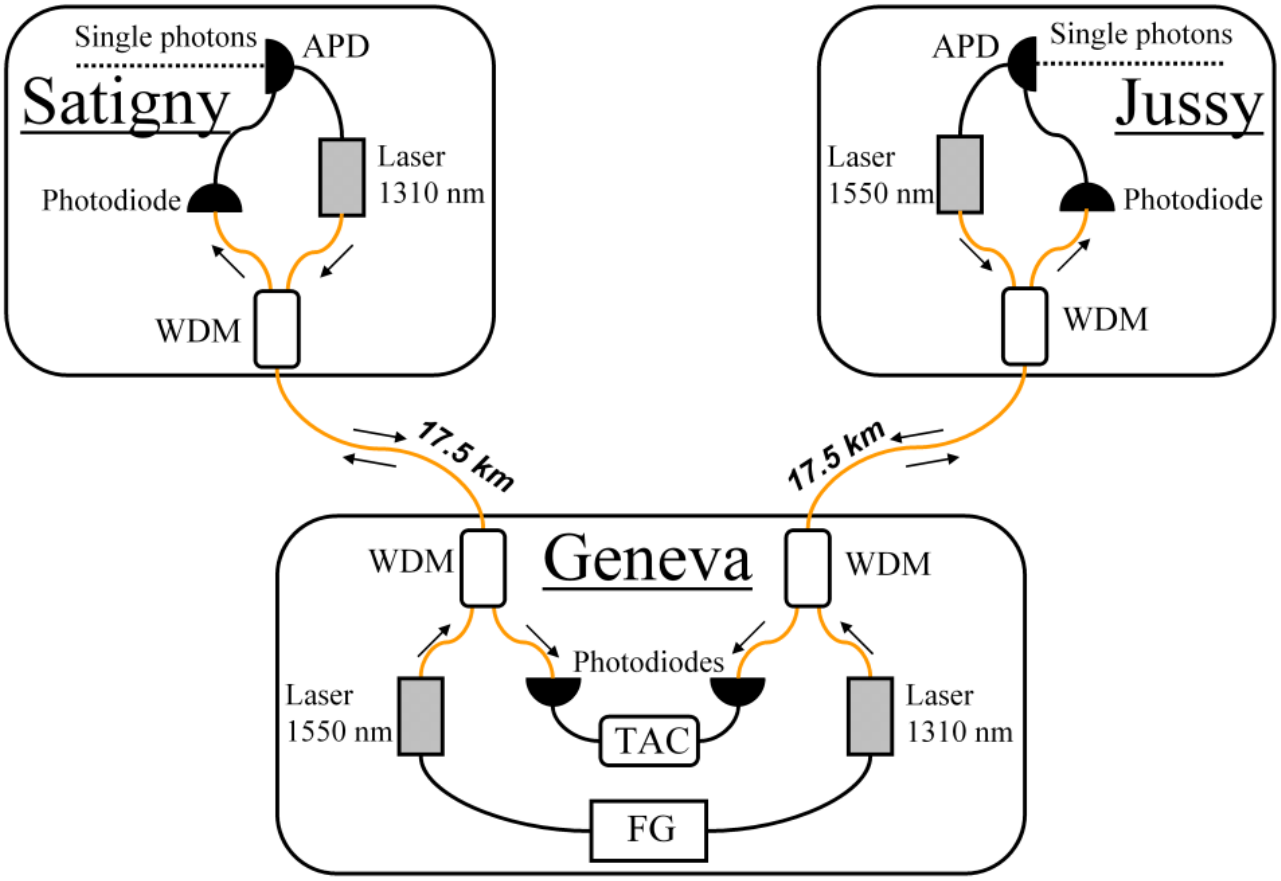

Supplementary Figure 2 | Experimental setup. Classical channels. A function generator (FG) sends a trigger signal of 1 MHz to two lasers. The optical signals are sent through 17.5 km of optical fibers to their respective receiving stations where they are detected by p-i-n photodiodes. The single-photon detectors are triggered by these signals and detection events are sent back to Geneva using the same fibers. WDMs and different laser wavelengths ensure the separation of the signals.

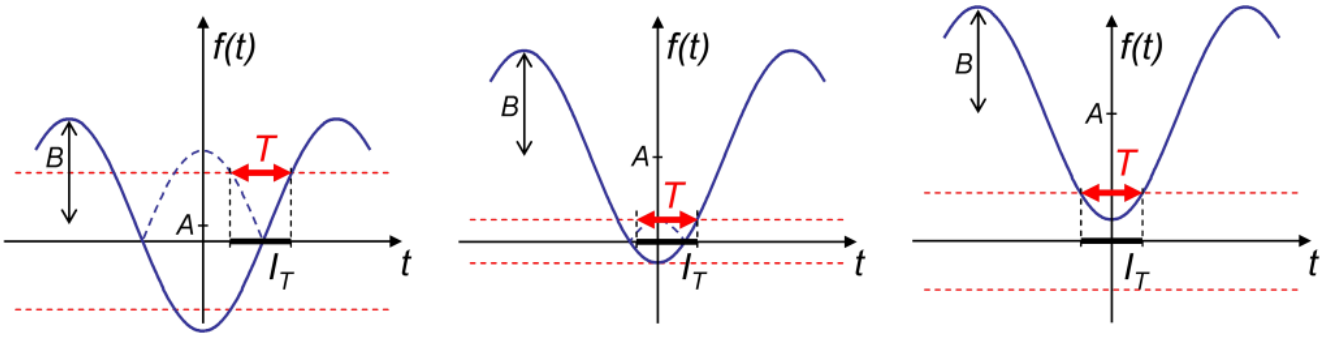

Supplementary Figure 3 | Upper bounds for $|f(t)|$ during an interval I_T of length T. Three cases for the analysis of $f(t) = A - B\cos\omega t$, depending on A and B.

Supplementary Discussion - Experiment

The experimental setup

These are the details of our experimental setup (see Supplementary Figure 1). The laser is a cw single mode external cavity diode laser (2.7 mW at 785.2 nm). It pumps a PPLN (Periodically Poled Lithium Niobate, $LiNbO_3$) nonlinear waveguide (HC Photonics) that creates pairs of photons through the process of spontaneous parametric down-conversion. All the guided light at 785.2 nm is blocked with a Silicon filter (F). The photon pairs are separated with two circulators and two fiber Bragg gratings (FBG). The first FBG reflects the photons at 1573.0 nm ($\Delta\lambda$=1.0 nm) and transmits all the other wavelengths. The second FBG reflects the photons at 1567.8 nm ($\Delta\lambda$=1.0 nm). The photons are sent to their respective receiving stations through standard communication optical fibers.

The fibered Michelson interferometers have arms of different lengths. The path-length difference is the same in both of them (l=267 mm or τ=1.3 ns). This is much shorter than the coherence length of the pump laser (l=23 m), allowing one to detect an entangled state when both photons pass through the same arm at their respective interferometers. At the same time, this is much longer than the coherence length of the single photons (l=2.47 mm), so there is no single-photon interference, and no phase-dependent variations in the single rates are observed. To compensate for birefringence effects in the arms of the interferometers (i.e. to stabilize polarization), Faraday mirrors (FM) are used.

The photons are detected by single-photon InGaAs avalanche photodiodes (APD) (id Quantique, id201). The quantum efficiency is 10% and the dead time is 10 μs. The photodiodes are operated in the gated mode with a repetition frequency of 1 MHz and a gate width of 100 ns. The measured single count rates for the detectors at Satigny and Jussy were 5.0 and 4.1 kHz, including 0.7 and 1.1 kHz of dark counts, respectively. A trigger signal is sent from Geneva to both detectors so as to open the gates synchronously. This improves the chances of having a coincidence detection. Each time the single-photon APDs detect an event, a classical optical signal is sent back to Geneva, where it is detected by a p-i-n photodiode and then sent to a time-to-amplitude-converter (TAC) that takes one of the signals as start and the other as the stop, measuring the difference in their arrival times. Coincidences in the arrival times between events coming from different detectors indicate that those photons passed either through the short-short or the long-long paths in the interferometers. The other two non-interfering possibilities (photons that passed through different arms − short-long or long-short paths) are discarded using a discriminator with a narrow window (600 ps).

The same fibers are used to send the trigger signal to the APDs and the detection signal back to Geneva. These are the classical channels shown in detail in Supplementary Figure 2. In the classical channels, the lasers at both ends of the fibers have different wavelengths (1550 nm and 1310 nm) and Wavelength Division Multiplexers (WDM) are used to separate the signals. These fibers are not the same ones that send the single-photons to the APDS (quantum channels in Supplementary Figure 1).

During each run of the experiment we continuously monitored both the single count rates (as a check of the stability of the entire setup) and the coincidence count rate. The average coincidence rate was 33 coinc./min. and the number of accidental coincidences 2.5 coinc./min.

The phase scan

To change the temperature and scan the phase in one of the interferometers, a voltage ramp is applied to its temperature controller. The temperature decreases regularly for several hours and is then heated quickly at the end of the ramp. This process was repeated during several days. The end of the cooling ramp stops the phase scan for several minutes making impossible to obtain arbitrarily long measurements of uninterrupted fringes.

The bound for V_{QI} is higher for shorter fringe periods T. To reduce the time T, one should increase the rate of the phase scan (more degrees per unit of time). Unfortunately, with a higher rate, the number of coincidences per minute diminishes, hence, the slope of the temperature ramp was adjusted so as to obtain a compromise period of T=360s.

The visibility fit

Long measurements of interference fringes with short fringe periods are usually very difficult to fit continously because slight variations in the period of the fringes can hinder the whole fit. To calculate the visibility values shown in Figure 4 of the article, we used a sinusoidal fit with an approximate length of one and a half fringes. This fit was displaced one point at a time throughout the entire measurement, fitting all the fringes. In a few cases, a fit gave a visibility value that differed considerably from the values given by the fits preceding it and following it. Two consecutive fits only differ by one point and visibility only has meaning when at least one fringe is involved, therefore this could not be due to a change in the visibility but instead because of an artifact of the fitting program. Taking the median of the ten values (less than a fringe) around each point and doing this for all the points of the measurement, we obtained the visibility values for all the interference fringes.

Supplementary Discussion - Theory

An expression for $\beta_\parallel(t)$

We denote by α the angle between the x-y equatorial plane and the direction A-B (see Figure 1). The unit vector $\mathbf{e}_{AB}$ in the A-B axis has a fixed component along the z direction, and a component in the x-y plane that rotates with an angular velocity ω: $\mathbf{e}_{AB}(t) = \sin\alpha\,\mathbf{e}_z + \cos\alpha\,\mathbf{e}_{xy}(t)$.

The speed $\mathbf{v}$ (or $\boldsymbol{\beta} = \mathbf{v}/c$) of the Earth frame in frame F can also be decomposed along the z axis and in the x-y plane: $\boldsymbol{\beta} = \beta\cos\chi\,\mathbf{e}_z + \beta\sin\chi\,\mathbf{e}^F_{xy}$.

By choosing the origin of time such that $\mathbf{e}_{xy}(t)\cdot\mathbf{e}^F_{xy} = \cos\omega t$, one gets:

$$\begin{aligned}\beta_\parallel(t) &= \boldsymbol{\beta}\cdot\mathbf{e}_{AB}(t)\\ &= \beta\cos\chi\sin\alpha + \beta\sin\chi\cos\alpha\cos\omega t\ .\end{aligned} \tag{1}$$

Upper bounds for $|\beta_\parallel(t)|$ during a period of time T

Consider, as a case study, the function $f(t) = A - B\cos\omega t$, for two parameters $A, B \in \mathbb{R}$.

For a given $T > 0$ (such that $\omega T < \pi$), we want to find an interval I_T of length T, during which we can upper bound $f(t)$ by the smallest possible value. A rigorous analysis gives the following results, where three cases must be distinguished (see Supplementary Figure 3 for a schematic representation of the three cases):

- If $|A| \le |B|\cos^2\frac{\omega T}{2}$, then there exists I_T, such that for all $t \in I_T$,

$$\begin{aligned}|f(t)| &\le \sqrt{B^2\sin^2\frac{\omega T}{2} - A^2\tan^2\frac{\omega T}{2}}\\ &\le \sqrt{B^2 - A^2}\,\frac{\omega T}{2}\ .\end{aligned} \tag{2}$$

- If $|B|\cos^2\frac{\omega T}{2} \le |A| \le |B|\cos^2\frac{\omega T}{4}$, then there exists I_T, such that for all $t \in I_T$,

$$|f(t)| \le |B| - |A|\ . \tag{3}$$

- If $|A| \ge |B|\cos^2\frac{\omega T}{4}$, then there exists I_T, such that for all $t \in I_T$,

$$|f(t)| \le |A| - |B|\cos\frac{\omega T}{2}\ . \tag{4}$$

For $A = \beta\cos\chi\sin\alpha$ and $B = -\beta\sin\chi\cos\alpha$, we get $f(t) = \beta_\parallel(t)$, to which we can apply the previous results. The bound (2) being also valid in the second case above, we grouped the first two cases to simplify the discussion, and thus obtained the two cases mentioned in the text of the Letter. Note that, since in our experiment we have $\omega T \ll 1$, the second case above is actually negligible.

Purification of Single-Photon Entanglement

D. Salart,[1] O. Landry,[1] N. Sangouard,[1] N. Gisin,[1] H. Herrmann,[2] B. Sanguinetti,[1] C. Simon,[1,*] W. Sohler,[2] R. T. Thew,[1] A. Thomas,[2] and H. Zbinden[1]

[1]*Group of Applied Physics, University of Geneva, 20, Rue de l'Ecole de Médecine, CH-1211 Geneva 4, Switzerland*
[2]*Universität Paderborn, Fakultät für Naturwissenschaften, Department Physik, Warburger Straße 100 33098 Paderborn, Germany*
(Received 25 January 2010; revised manuscript received 26 March 2010; published 6 May 2010)

Single-photon entanglement is a simple form of entanglement that exists between two spatial modes sharing a single photon. Despite its elementary form, it provides a resource as useful as polarization-entangled photons and it can be used for quantum teleportation and entanglement swapping operations. Here, we report the first experiment where single-photon entanglement is purified with a simple linear-optics based protocol. In addition to its conceptual interest, this result might find applications in long distance quantum communication based on quantum repeaters.

DOI: 10.1103/PhysRevLett.104.180504 PACS numbers: 03.67.Bg, 42.50.Dv, 42.50.Ex

Entanglement purification provides a fascinating conceptual viewpoint to gain insight into the properties of entanglement. It can be used for the quantification of entanglement in bipartite systems [1]. It may also be useful in practical applications, e.g., in the context of long distance quantum communication where the direct transmission of photons through an optical fiber is limited by losses and the no-cloning theorem. This can be overcome using quantum repeaters [2], which require the creation of entanglement over short links, the storage of entangled states within these links, and entanglement swapping operations to distribute entangled states over longer distances. In practice, these operations introduce errors, limiting the number of links that can be used. While the most immediate goal of outperforming the direct transmission may not need purification, the entanglement distribution within future quantum networks requires a larger number of links, necessitating several purification operations [3].

Initial proposals by Bennett *et al.* [4] and Deutsch *et al.* [5] for entanglement purification were expressed in terms of quantum gates. For practical applications, e.g., in the frame of quantum repeaters, it is important to keep implementations as simple as possible. For example, the protocol presented in Ref. [6] and implemented as reported in Ref. [7] requires linear optical elements only, and can easily be integrated into quantum repeater architectures. However, this last proposal is suited to the purification of polarization-entangled pairs of photons whereas many attractive quantum repeater protocols [8–10] and related experiments [11,12] use single-photon entanglement, i.e., entanglement of the form $|1\rangle_A|0\rangle_B + |0\rangle_A|1\rangle_B$, where two modes A and B share a single photon. First, these repeaters are rather simple: they require significantly fewer resources than other protocols and are thus less sensitive to memory and photon detector inefficiencies [3]. Furthermore, these quantum repeaters are efficient since they offer high entanglement distribution rates when combined with temporal multiplexing [9]. The main drawback of protocols based on single-photon detections is that, unlike protocols based on two-photon detections, they are interferometrically sensitive to path length fluctuations [13] that are at the origin of phase errors. An active stabilization system, such as the one reported in [14], would be required. However, remaining path length fluctuations and additional phase noise coming from unfaithful quantum memories and imperfections in entanglement swapping operations would likely require purification. Here, we report the first experimental implementation of a protocol for phase-error purification of single-photon entanglement based on linear optics.

The principle of purification for phase errors (see Ref. [15] for details) can be illustrated as follows. Alice and Bob, two protagonists located at remote locations A and B respectively, wish to share a maximally entangled state $\psi_+^{ab} = \frac{1}{\sqrt{2}}(|1\rangle_A|0\rangle_B + |0\rangle_A|1\rangle_B) \equiv \frac{1}{\sqrt{2}}(a^\dagger + b^\dagger)|0\rangle$, but due to phase errors, they share a state which has an admixture of the singlet state ψ_-^{ab}

$$\rho_{ab} = F|\psi_+^{ab}\rangle\langle\psi_+^{ab}| + (1-F)|\psi_-^{ab}\rangle\langle\psi_-^{ab}|. \quad (1)$$

F is the fidelity of the shared state: if $F = 1/2$, the phase information is lost and no entanglement is left while in the case where $F = 1$, the state is maximally entangled. Note that these phase errors are the most important. The empty component $|0\rangle_A|0\rangle_B$ does not affect the fidelity of the distributed state since the final step of single-photon protocols postselects the cases where there was a photon in the output state [8]. The multiphoton components $|1\rangle_A|1\rangle_B$ can be greatly reduced using specific architectures [10].

Suppose that Alice and Bob share two copies of the state described by (1), $\rho_{a_1b_1}$ with fidelity F_1 and $\rho_{a_2b_2}$ with fidelity F_2 (see Fig. 1). Alice and Bob both perform unitary transformations on their modes a_1, a_2 and b_1, b_2 respectively: Alice combines the two modes a_1, a_2 on a beam splitter with an intensity transmission of 85% and Bob uses a beam splitter with an intensity transmission of 15%. The detection of a single photon by Alice in mode d_a (or by Bob in mode d_b), projects the modes $\tilde{a}$, $\tilde{b}$ on a mixed state

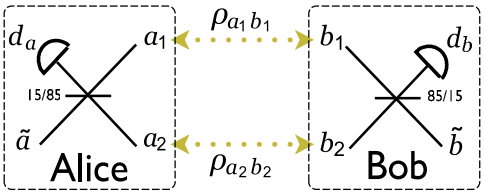

FIG. 1 (color online). Scheme for entanglement purification of single-photon entanglement. Alice and Bob share two entangled single-photon states $\rho_{a_1 b_1}$, $\rho_{a_2 b_2}$ [of the form given in Eq. (1)] with fidelity F_1 and F_2, respectively. While Alice combines the modes a_1 and a_2 on a 15/85 beam splitter, Bob couples the modes b_1 and b_2 on a 85/15 beam splitter. The detection of one photon in either d_a or d_b projects the modes $\tilde{a}$ and $\tilde{b}$ into a single-photon entangled state $\rho_{\tilde{a}\tilde{b}}$ with higher fidelity $\tilde{F}$.

$\rho_{\tilde{a}\tilde{b}}$ with fidelity [15]

$$\tilde{F} = \frac{F_1 F_2 + F_1/2 + F_2/2}{1 + F_1 F_2 + (1 - F_1)(1 - F_2)}. \qquad (2)$$

Remarkably, the state resulting from this simple operation is substantially purified. As an example, if errors are of the order of ϵ, i.e., $F_1 = F_2 = 1 - \epsilon$, the purification protocol divides them by a factor of 2, i.e., $\tilde{F} = 1 - \epsilon/2 + o(\epsilon^2)$. In quantum repeaters the error is approximately doubled with every level of entanglement swapping. The present protocol has the potential to significantly increase the number of possible levels, and thus the achievable distance. Furthermore, in principle, the protocol could be applied again to the already purified states, and this process could continue as long as there are entangled states remaining, obtaining an increasingly purified state at every step. Note that the success probability for the purification protocol is $p = \frac{1}{4}[1 + F_1 F_2 + (1 - F_1)(1 - F_2)]$ which is close to $1/2$ for values of F_1 and F_2 that are close to 1. Note also that the previously mentioned proposal [6] based on polarization entanglement squares the errors, i.e., $\tilde{F} = 1 - \epsilon^2 + o(\epsilon^3)$. We have shown that our scheme achieves the optimal fidelity (see Ref. [15] for a detailed discussion) for single-photon entanglement. This protocol reveals an intrinsic difference between single-photon entanglement and polarization-entangled photons.

The physics behind the purification is based on the interference of two modes sharing a single photon and on the bosonic character of indistinguishable photons. Single-photon interference requires a stable setup. Phase oscillations need to be kept under certain control in order to apply the purification protocol successfully. Indeed, there needs to be some initial entanglement left to purify. For a kilometer long interferometer, active stabilization would likely be required. In our experiment, where interferometer arms are 10 m long, phase oscillations are minimized by controlling the temperature. Indistinguishability of the photons demands a good overlap of the temporal, spectral, spatial and polarization modes of the photons. Thus, the successful construction and operation of an experimental setup that provided both indistinguishable photons and high visibility single-photon interference allows us, for the first time, to demonstrate the purification of single-photon entanglement.

The experimental setup is shown in Fig. 2. A Ti-indiffused 7 μm wide waveguide in 25 mm long periodically poled ($\Lambda = 9.15$ μm) lithium niobate (Ti:PPLN) operated at 43 °C—monomode around 1.5 μm wavelength—creates degenerate photon pairs through the process of spontaneous parametric down conversion. The periodicity of Λ has been chosen to obtain "type-II" quasi-phase-matching for orthogonally polarized signal and idler photons. The waveguide is pumped by a continuous-wave single-mode external cavity diode laser at 780 nm (Toptica DL100). After the waveguide, the remaining light from the pump laser is blocked by a silicon filter. The signal and idler photons, with a spectral width of 3 nm (full width at half maximum) centered at 1560 nm, both pass through the same narrowband filter with a bandwidth of 1.3 nm reducing their spectral distinguishability. The photons are then separated with a polarizing beam splitter (PBS) and coupled into single-mode optical fibers. Each photon is sent through a 50/50 coupler (BS1 and BS2) to prepare the two-mode entangled states $\rho_{a_1 b_1}$ and $\rho_{a_2 b_2}$. These states are then distributed between Alice and Bob. They each receive two modes, one from each entangled state, and combine them using couplers BS4 and BS5, respectively. These last two couplers are manual

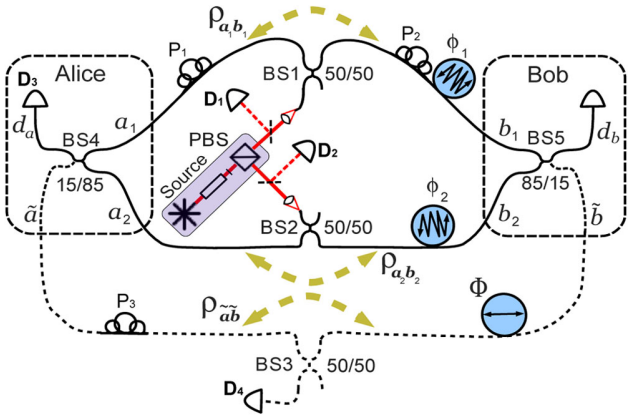

FIG. 2 (color online). Experimental setup. Pairs of orthogonally polarized photons are created by a waveguide-based source, separated by a PBS and coupled into optical fibers. Each photon passes through a 50/50 coupler (BS1 and BS2) to create two-mode entangled states $\rho_{a_1 b_1}$ and $\rho_{a_2 b_2}$. Alice and Bob each receive two modes, one from each state, and combine them using 15/85 couplers (BS4 and BS5). Conditional on the detection of one photon by either Alice or Bob, a purified single-photon entangled state $\rho_{\tilde{a}\tilde{b}}$ is created. The degree of entanglement is measured using the 50/50 coupler BS3. Two noise generators (ϕ_1 and ϕ_2) are used to reduce the fidelities F_1 and F_2 of $\rho_{a_1 b_1}$ and $\rho_{a_2 b_2}$, respectively. The phase Φ is scanned using a piezo to acquire an interferogram and thus estimate the fidelities.

variable-ratio evanescent wave couplers (Canadian Instrumentation & Research Ltd).

Finally, for all measurements we use two single-photon detectors: the heralding detector is a free-running InGaAs/InP avalanche photodiode with homemade electronics [16]. Depending on the measurement, this detector is at positions D_1, D_2 or D_3 in Fig. 2. The quantum efficiency is 10.2% with 1.3 kHz of dark counts for a temperature of $-50\,^{\circ}\mathrm{C}$ and a bias voltage of -48.5 V. Its *effective* efficiency decreases as the number of singles increases, since the detection rate is limited by a dead time of 31 μs. The triggered detector is an InGaAs avalanche photodiode (idQuantique, id200) working in gated mode and operated at an efficiency of 5.5%, 2.7×10^{-5} dark counts $\cdot\ \mathrm{ns}^{-1}$ and a dead time of 10 μs.

The efficiency of the photon pair source is determined by calculating the number of photon pairs that are created. We measure 15.5 kHz of singles at detector D_1, an effective detector efficiency of 5.3% and a transmission of 0.077 between the waveguide and detector D_1. We generate approximately 4×10^6 pairs $\cdot\ \mathrm{s}^{-1}$ for a spectral width of 1.3 nm from a pump power of 16 mW at 780 nm. This is equivalent to $p = 3.2 \times 10^{-3}$ pairs per detection time window of $\tau_d = 800$ ps. The detection time window is the FWHM of the coincidence peak and it depends primarily on the jitter of the single-photon detectors.

The degree of indistinguishability of the two photons can be measured through the visibility of the Hong-Ou-Mandel (HOM) dip [17]. If the photons were perfectly indistinguishable, the number of coincidences would be zero and the visibility of the HOM dip would be 100%. We have estimated, using a simple model with discrete modes, that the presented protocol requires overlaps between the distributions associated to the modes a_1, a_2, b_1 and b_2 above 90% to obtain a significant purification effect. The temporal overlap between the modes is achieved by adjusting the path lengths that each photon has to travel between the PBS and the couplers BS3, BS4, and BS5. The spectral overlap is ensured due to both photons passing through the same narrowband filter. The use of single-mode fibers guarantees the transverse spatial overlap. Lastly, the polarization is controlled using the polarization controllers shown in Fig. 2. After performing these adjustments, we observed a HOM dip with the extremely high visibility of $V_{\mathrm{dip}} = (C_{\mathrm{max}} - C_{\mathrm{min}})/C_{\mathrm{max}} = (99.0 \pm 0.3)\%$.

To determine the degree of entanglement for $\rho_{a_1 b_1}$, we measure the visibility V_1 of interference fringes. The visibility is a good measure of the fidelity $F_1 = (1 + V_1)/2$ of the state $\rho_{a_1 b_1}$ since we postselect the cases where there is at least one excitation in either a_1 or b_1 and since the probability of multipair emissions is low, as confirmed by the visibility of the HOM dip. To herald the creation of the state $\rho_{a_1 b_1}$ at coupler BS1, the photon reflected at the PBS is not sent to BS2 but detected by D_2. Its modes a_1, b_1 are sent to Alice and Bob, respectively, and then combined using the auxiliary measurement interferometer (depicted as dotted lines in Fig. 2) that leads to coupler BS3 and detected at D_4. The path chosen by the single photon is unknown, leading to interference fringes when the phase Φ of the interferometer is scanned. To scan this phase, we use a circular piezoelectric actuator with optical fiber coiled around it. A voltage ramp is applied to the piezo that progressively expands, stretching the fiber and changing the phase. To determine the degree of entanglement for $\rho_{a_2 b_2}$, the measurement is repeated, inverting the roles for the transmitted and reflected photons at the PBS. We measured the initial fidelity of $\rho_{a_1 b_1}$ as $F_1 = (97.8 \pm 0.2)\%$ while $\rho_{a_2 b_2}$ has a fidelity $F_2 = (97.7 \pm 0.2)\%$. The residual 2% is mainly due to path length instabilities (see the supplementary information in Ref. [18]).

This purification protocol works for a wide range of fidelities F_1 and F_2, but it is at fidelities close to $F_1 = F_2 = 76\%$ where the fidelity increase is greatest [15]. To reduce the initial fidelities, we generate noise in a controlled and reproducible way with two additional circular piezos (ϕ_1 for state $\rho_{a_1 b_1}$ and ϕ_2 for state $\rho_{a_2 b_2}$) that vibrate at a frequency much higher than the integration time of the measurement. This noise is independently generated for each piezo. We chose a function that reproduces the Gaussian phase-noise distribution in a fiber, as observed in real world networks [13]. Interference fringes measured in one of the entangled states and the reduction of the fidelity due to the noise generation are shown in Fig. 3(a). After applying the noise, the fidelities reduce to $F_1 = (75.1 \pm 0.8)\%$ and $F_2 = (75.0 \pm 0.7)\%$.

To prepare the purified state, the variable couplers BS4 and BS5 are adjusted to the intensity transmissions re-

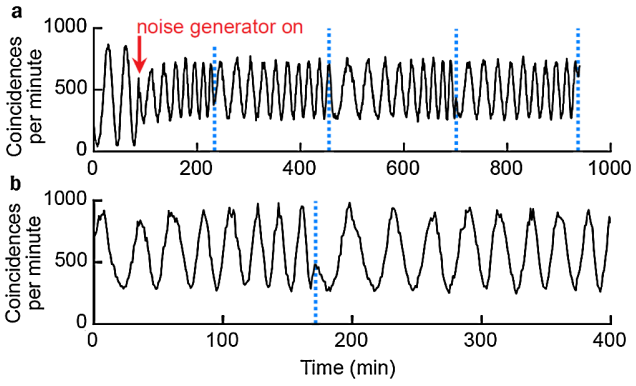

FIG. 3 (color online). Raw interference fringes observed while the phase Φ is being scanned. (a) Coincidences between detectors D_1 (herald) and D_4 corresponding to the state $\rho_{a_2 b_2}$. Initially, the fidelity is $F_2 = (97.7 \pm 0.2)\%$. When the noise generator ϕ_2 is switched on, the fidelity decreases to $F_2 = (75.0 \pm 0.7)\%$. (b) Coincidences between detectors D_3 and D_4 corresponding to the purified state $\rho_{\tilde{a}\tilde{b}}$. While both noise generators are on, the fidelity is $\tilde{F} = (79.6 \pm 1.1)\%$. These values are obtained after the subtraction of accidental coincidences due to dark counts. Even when they are not subtracted, a definite purification effect can still be observed. The vertical lines mark every time the voltage ramp reaches its end, reversing the scan direction.

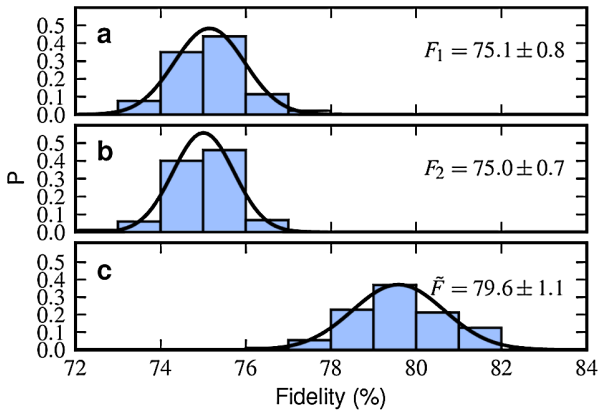

FIG. 4 (color online). Distribution of the fidelity measurements. Probability densities P as a function of the measured fidelities for (a) state $\rho_{a_1 b_1}$, (b) state $\rho_{a_2 b_2}$ and (c) the purified state $\rho_{\tilde{a}\tilde{b}}$. The corresponding mean fidelity and standard deviation are given next to each distribution. The curves are Gaussian functions with the same mean and σ as the sample data. The number of bins chosen is the optimal one using Scott's principle [22]. The agreement with the histogram can be seen by the fact that the fitted curve passes through the center of most histogram bars.

quired to apply the purification protocol [15], corresponding to 85% for Alice and 15% for Bob (or vice versa). Modes a_1 and a_2 are combined by Alice to form modes $\tilde{a}$ and d_a, while modes b_1 and b_2 are combined by Bob to form modes $\tilde{b}$ and d_b. Conditioned on the detection of one photon at d_a (with detector D_3), modes $\tilde{a}$ and $\tilde{b}$ become purified. To verify this, they are combined at coupler BS3 and detected at D_4. Again, because we cannot know which path the photons have taken, interference fringes are observed when the phase Φ is scanned [see Fig. 3(b)]. As before, the fidelity $\tilde{F}$ of the state $\rho_{\tilde{a}\tilde{b}}$ is deduced from the visibility of the fringes.

For each of the entangled states ($\rho_{a_1 b_1}$, $\rho_{a_2 b_2}$ and $\rho_{\tilde{a}\tilde{b}}$), measurements of several interference fringes were obtained. Using sequential sinusoidal fits of approximately two periods, we calculated the fidelities for all fringes. The resulting distributions of fidelity values are represented in Fig. 4. From each set of values, the mean fidelities F_1, F_2, and $\tilde{F}$ were calculated. The given uncertainty values are the standard deviations (σ) associated with each distribution [18].

After the implementation of the purification protocol, we obtain a state $\rho_{\tilde{a}\tilde{b}}$ with fidelity $\tilde{F} = (79.6 \pm 1.1)\%$. The improvement in the degree of entanglement, taken as the difference between $\tilde{F}$ and F_1, is as high as 4.5%. Note that it has been shown in Ref. [15] that the optimal theoretical value is of 5.7%. We believe that the remaining 1.2% is due to phase fluctuations of modes and to the uncertainty in the transmission of variable couplers [18]. As shown in Fig. 4, the overlap between the distributions of initial and purified fidelity values is negligible, leaving no doubt about the influence of the purification effect.

Single-photon entanglement has been at the heart of a lively debate [19,20]. Part of the controversy has been solved by mapping single-photon entanglement into two atomic ensembles and by revealing the entanglement between these ensembles [12]. Note also that entanglement between four modes sharing a single photon has been characterized by direct measurements of the optical modes [21]. Our experiment further shows that single-photon entanglement can be purified using linear optics. Looking further ahead, this simple protocol could be useful in the context of quantum repeaters.

We thank C. Barreiro and J.-D. Gautier for technical support and H. de Riedmatten for his insightful comments and careful reading of the manuscript. This work was supported by the Swiss NCCR Quantum Photonics and the European Union projects QAP and ERC-AG QORE.

*Present address: Institute for Quantum Information Science and Department of Physics and Astronomy, University of Calgary, 2500 University Drive NW, Calgary T2N 1N4, Alberta, Canada.

[1] R. Horodecki *et al.*, Rev. Mod. Phys. **81**, 865 (2009).
[2] H.-J. Briegel *et al.*, Phys. Rev. Lett. **81**, 5932 (1998).
[3] N. Sangouard *et al.*, arXiv:0906.2699.
[4] C. H. Bennett *et al.*, Phys. Rev. Lett. **76**, 722 (1996).
[5] D. Deutsch *et al.*, Phys. Rev. Lett. **77**, 2818 (1996).
[6] J.-W. Pan *et al.*, Nature (London) **410**, 1067 (2001).
[7] J.-W. Pan *et al.*, Nature (London) **423**, 417 (2003).
[8] L.-M. Duan *et al.*, Nature (London) **414**, 413 (2001).
[9] C. Simon *et al.*, Phys. Rev. Lett. **98**, 190503 (2007).
[10] N. Sangouard *et al.*, Phys. Rev. A **76**, 050301(R) (2007).
[11] C.-W. Chou *et al.*, Nature (London) **438**, 828 (2005); C.-W. Chou *et al.*, Science **316**, 1316 (2007).
[12] K. S. Choi *et al.*, Nature (London) **452**, 67 (2008).
[13] J. Minář *et al.*, Phys. Rev. A **77**, 052325 (2008).
[14] S.-B. Cho, and T.-G. Noh, Opt. Express **17**, 19027 (2009).
[15] N. Sangouard *et al.*, Phys. Rev. A **78**, 050301(R) (2008).
[16] R. T. Thew *et al.*, Appl. Phys. Lett. **91**, 201114 (2007).
[17] C. K. Hong, Z. Y. Ou, and L. Mandel, Phys. Rev. Lett. **59**, 2044 (1987).
[18] See supplementary material at http://link.aps.org/supplemental/10.1103/PhysRevLett.104.180504 for more detailed information about the measurement procedure, the data analysis, accidental coincidences and the imperfect HOM dip visibility and fidelities.
[19] S. M. Tan, D. F. Walls, and M. J. Collett, Phys. Rev. Lett. **66**, 252 (1991).
[20] S. J. van Enk, Phys. Rev. A **72**, 064306 (2005) and references therein.
[21] S. B. Papp *et al.*, Science **324**, 764 (2009).
[22] D. W. Scott, Biometrika **66**, 605 (1979).